

Resistance experiments on a systematic series of high speed displacement monohull and catamaran forms in shallow water.

A.F. Molland, P.A. Wilson and D.J. Taunton.

Ship Science Report No. 127
University of Southampton

2003

Contents

Nomenclature.....	2
1 Introduction.....	3
2 Description of Models.....	3
3 Facilities and Tests.....	4
3.1 General.....	4
3.2 Wave Pattern Resistance.....	4
3.3 Trim and Sinkage Measurements.....	5
4 Data Reduction and Correction.....	5
4.1 Coefficients.....	5
4.2 Temperature Correction.....	5
4.3 Resistance due to Turbulence Studs.....	6
4.4 Wetted Surface Area.....	6
5 Presentation of Data.....	6
6 Discussion of Results.....	7
6.1 Total resistance and wave pattern resistance.....	7
6.2 Running sinkage and trim.....	8
6.3 Wave properties.....	9
6.3.1 General.....	9
6.3.2 Distribution of wave resistance (energy).....	9
7 Conclusions.....	10
Acknowledgements.....	10
References.....	11
Tables.....	12
Figures.....	14

Nomenclature

Demihull: One of the hulls which make up the catamaran.

A	Wetted surface area (demihull) [m^2]
Fn_L	Froude Number [$V(gL)^{-1/2}$]
Fn_H	Depth Froude Number [$V(gh)^{-1/2}$]
H	Water depth [m]
L	Length of model on waterline [m]
S	Separation between catamaran demihull centrelines [m]
T	Wave period [s]
V	Ship speed [ms^{-1}]
Y	Distance of wave cut from centreline of model [m]
C_F	Coefficient of frictional resistance [ITTC'57 correlation line]
C_R	Coefficient of residuary resistance [$R_R/(\frac{1}{2}\rho AV^2)$]
C_T	Coefficient of total wave resistance [$R_T/(\frac{1}{2}\rho AV^2)$]
C_{WP}	Coefficient of wave pattern resistance [$R_{WP}/(\frac{1}{2}\rho AV^2)$]
R_R	Residuary resistance [N]
R_T	Total resistance [N]
R_{WP}	Wave pattern resistance [N]
Volume of displacement (demihull)	[m^3]
(1+k)	Form factor
β	Viscous resistance interference factor
τ	Wave resistance interference factor
g	Acceleration due to gravity [9.81ms^{-2}]
ρ	Density of water [kgm^{-3}]
θ	Wave angle [$^\circ$]

1 Introduction

Work on the resistance of high speed displacement catamarans has been ongoing over a number of years at the University of Southampton [1-4] in an effort to improve the understanding of their resistance components, seakeeping performance and to provide design and validation data.

This report describes an extensive series of wash wave measurements for monohull and catamarans models travelling in shallow water. The models were chosen from the series used in [1, 4], for which extensive resistance and wave characteristics in deep water are available.

The tests covered a range of length: displacement ratios $[L/\nabla^{1/3}]$ and catamaran separation: length ratios $[S/L]$ at two shallow water depths. The model speeds and water depths tested led to a range of Froude Numbers (based on length) of $Fn_L = 0.25 - 1.2$ and a Froude Number (based on water depth) of $Fn_H = 0.5 - 3.2$. The experiments entailed the measurement of wave profiles at seven transverse positions, model total resistance, sinkage and trim. Comprehensive reports on the test data for the wave profiles are given in [5-7].

The work described forms part of a wider research programme, funded by EPSRC and industry and managed by Marinetech South Ltd over a two year period, which includes the development of theoretical methods for the prediction of the wash and wave resistance of catamarans. The theoretical work is the subject of a separate report [8]

2 Description of Models

Details of the models used in this investigation are given in Table 1.

The models were constructed using an epoxy-foam sandwich skin. Models 4b, 5b and 5s are 1.6m in length. The length of model 6b was increased to 2.1m in order to achieve a satisfactory weight – displacement balance.

It should be noted that Models 4b, 5b and 6b had already been used for resistance tests in deep water and their results published in [9]. Some of the results for these models are used in the present report for comparison and discussion.

The models were of round bilge form with transom sterns, Figure 1, and were derived from the NPL round bilge series [10] and the Series 64 round bilge series [11]. These hulls broadly represent the underwater form of a number of catamarans in service or currently under construction. The models were first tested as monohulls and then in catamaran configurations with Separation: Length ratios (S/L) of 0.2 and 0.4.

The model towing force was in the horizontal direction. The towing point in all cases was situated at the longitudinal centre of gravity and at a height of 2/3 of the draught above the baseline. No compensation was made for the vertical separation of the tow point and the

propeller thrust line. The tow fitting allowed free movement in sinkage and trim whilst movements in surge, sway, roll and yaw were restrained. The models were fitted with turbulence stimulation comprising trip studs of 3.2mm diameter and 2.5mm height at a spacing of 25mm. The studs were situated 37.5mm aft of the stem. No underwater appendages were attached to the models. The weight of the towpost was 2.045 Kg.

3 Facilities and Tests

3.1 General

The model experiments were carried out in the GKN-Westland Aerospace test tank on the Isle of Wight, which has the following principal particulars:

Length	:	200m
Breadth	:	4.6m
Water depth	:	1.7m
Maximum carriage speed	:	14m s ⁻¹

In the current tests, water depths of 400mm and 200mm were used.

The tank has a manned carriage which is equipped with a dynamometer for measuring model total resistance together with various computer and instrumentation facilities for automated data acquisition. For these shallow water tests a Wolfson Unit MTIA dynamometer was used which was attached to an aluminium alloy frame situated under the main carriage.

Calm water total resistance, running trim, sinkage and wave pattern measurements were carried out for all the models. All tests were carried out where possible over a speed range of 1m s⁻¹ to 4m s⁻¹ corresponding to a length Froude Number range of F_{nL} 0.25 to 1.0 and a depth Froude Number range F_{nH} 0.2 to 2.8. Over the length Froude Number range 0.25 to 1.0, the corresponding Reynold's Number range for the models was $1.54 \cdot 10^6$ to $6.18 \cdot 10^6$ for the 1.6m models and $2.03 \cdot 10^6$ to $8.11 \cdot 10^6$ for the 2.1m model.

3.2 Wave Pattern Resistance

Extensive wave profile measurements were carried out to establish a wide database of wash wave characteristics in shallow water, which would be suitable for design and validation purposes. Such an extensive set of wave data would also facilitate the description of the near field wave pattern in three dimensions from the experimental results and facilitate the interpolation of the experimental data at various transverse positions. A wave pattern analysis based on a combined matrix solution of four longitudinal wave cuts was used to determine the wave pattern resistance. A full description of the apparatus and analysis method is given in [1].

The wave profiles were measured using resistance type wave probes with a length of 300mm coupled to a Churchill wave probe monitor. The data were acquired and stored using a laptop computer situated at the side of the tank adjacent to the wave probes. The signals were

acquired at a sampling rate of 100Hz. The acquisition program allowed a run time of up to 40 seconds to be used.

During each test run, seven longitudinal wave profiles were measured, with transverse positions (Y) relative to the centreline of the tank as shown in Figures 1b, 1c and 1d. Relative to model length, these positions have values of Y/L =0.43, 0.55, 0.68, 0.80, 0.93, 1.05 and 1.18 for Models 4b, 5b and 5s and Y/L=0.33, 0.42, 0.52, 0.61, 0.71, 0.80 and 0.90 for Model 6b. The longitudinal position of the wave probes in the tank are shown in Figure 1d. This position allowed adequate time for the wave system to settle before measurements commenced.

3.3 Trim and Sinkage Measurements

Trim and sinkage were monitored for all of the tests. Trim (positive bow up) was measured by means of a potentiometer mounted on the tow fitting; accuracy of the measurement was within $\pm 0.05^\circ$. Sinkage (positive downwards) was measured by means of a potentiometer and a track on the towpost; accuracy of the measurement was within $\pm 0.1\text{mm}$.

4 Data Reduction and Correction

4.1 Coefficients

All resistance data were reduced to coefficient form using fresh water density ($\rho=1000\text{ kgm}^3$), static wetted surface area (A) and model speed (U):

$$\text{Resistance Coefficient} = \frac{\text{Resistance}}{\frac{1}{2}\rho AU^2} \quad (1)$$

Noting A is the wetted area of both demihulls in the case of the catamaran.

Corrections were applied as necessary to the measured data and these are described in the following sections:

4.2 Temperature Correction

During the tests the water temperature varied from 18°C to 20°C . The total resistance measurements were corrected to the standard temperature of 15°C by modifying the frictional resistance component. The correction which has been applied is as follows:

$$C_{T_{15}} = C_{T_{\text{test}}} - C_{F_{\text{test}}} + C_{F_{15}} \quad (2)$$

The correction should be slightly larger due to the form factor being greater than unity. However, the correction is in any case small and the above equation is considered to be sufficiently accurate.

4.3 Resistance due to Turbulence Studs

Turbulence studs were attached to all the models as described in Section 2. A detailed investigation of their influence on model drag was carried out, and is described in [9]. It was found that, whilst there was additional drag on the studs, this is to a certain extent negated by the laminar region upstream and the boundary layer momentum thickness increase downstream due to the studs.

4.4 Wetted Surface Area

Static wetted surface area was used to non-dimensionalise the resistance measurements. A detailed investigation into the use of running wetted surface area is described in [9]. The conclusions in [9] indicate that whilst the use of running wetted surface might provide a better understanding of the physical components of resistance, the use of static wetted area does not have a significant effect on model to ship extrapolation providing both model and full scale coefficients are based on static wetted surface area. Running wetted surface area is difficult to measure experimentally in a routine manner, and will not be available for a new design. From a practical viewpoint it is necessary to use the static wetted surface area, and it has therefore been applied in the current work.

5 Presentation of Data

The basic presentation of the experimental resistance data is similar to that used in the earlier work, [1, 2] and is summarised as follows.

For monohulls:

$$C_T = (1+k)C_F + C_W \quad (3)$$

and for catamarans:

$$C_T = (1+\beta k)C_F + \tau C_W \quad (4)$$

where C_F is derived from the ITTC'57 correlation line, C_W is the wave resistance coefficient for the demihull in isolation, $(1+k)$ is the form factor for the demihull in isolation, β is a viscous resistance interference factor and τ is the wave resistance interference factor.

The measured experimental resistance data are presented in Figs. 2 to 25. In these diagrams the wave pattern resistance C_{WP} is plotted downward from the total resistance C_T , in the form $(C_T - C_{WP})$. The estimates of $(1+k)$ and $(1+\beta k)$ derived from the deep water tests, [2-4], are also shown on the diagrams. These lines are set to the lower envelope of the $(C_T - C_{WP})$ curves when they settle at an approximately constant level above the ITTC C_F correlation line

at the higher Froude Numbers. The values of $(1+k)$ for the monohulls and $(1+\beta k)$ for the catamarans are, for practical design purposes, assumed to remain constant over the speed range.

From a practical viewpoint it is not necessary to confine the user to the particular values of $(1+k)$ and $(1+\beta k)$ derived in this work. Residuary resistance coefficients C_R , derived from $(C_T - C_F)$, have been calculated from the experimental data and are tabulated in Table 2 to 5. This provides the data in a form suitable for practical powering applications. The user is able to choose a suitable $(1+k)$ or $(1+\beta k)$ from an appropriate source and, for an estimate of the ship total resistance coefficient, it can be shown that:

for monohulls:

$$C_{Tship} = C_{Fship} + C_{Rmodel} - k(C_{Fmodel} - C_{Fship}) \quad (5)$$

and for catamarans:

$$C_{Tship} = C_{Fship} + C_{Rmodel} - \beta k(C_{Fmodel} - C_{Fship}) \quad (6)$$

noting that C_{Fmodel} (derived using the ITTC'57 correlation line) will use the model length from which the C_R was derived (see Table 1).

Figs. 26 to 29 show the influence on the total resistance of $L/\nabla^{1/3}$, S/L , water depth and hull shape. The results of the running sinkage and trim measurements are presented in Figs. 30 to 45. Due to the number of measurements and wave cuts during a run, the overall number of runs per case were limited. As a result, and in order to provide clarity of interpretation the lines through the data in Figs. 26 to 45 are drawn point to point, rather than attempting to fair the data.

A typical example of the multiple wave cuts measured during one run are shown in Fig. 46. Fig. 47 shows the angle of wave propagation derived from the wave measurements.

The distributions of wave resistance/ energy against component wave angle are shown in Figs. 48 to 173. In some cases it was not possible to determine the distribution of wave resistance from the analysis of the longitudinal cuts so these results are not included.

6 Discussion of Results

6.1 Total resistance and wave pattern resistance

The results of the total resistance and wave pattern measurements are shown in Figs. 2 to 25. The total resistance values show a distinct increase near the critical depth Froude Number ($F_{nH} = 1.0$). This increase is larger for the smaller water depth (200mm). This is likely to be due to the smaller clearance under the keel for the smaller water depth leading to larger interference. At sub-critical and supercritical speeds the resistance values are very similar and effectively independent of water depth. Similar results were obtained by Dand, [12].

The total viscous resistance $(1+k)C_F$ or $(1+\beta k)C_F$ using the values of $(1+k)$ and $(1+\beta k)$ derived from the deep water results, [2-4], are also shown on the figures. It is interesting to note that at the higher supercritical speeds, the shallow water resistance coefficients are very similar to the deep water results, i.e. the $(C_T - C_{WP})$ curves are at the same level as the deep water $(1+k)C_F$ and $(1+\beta k)C_F$ values.

The wave pattern measurements are plotted downwards from the total resistance values. Like the earlier deep water tests, the results display a hump (or decrease in measured wave pattern resistance) in the length Froude Number range 0.3 to 0.5 before settling down at an approximately constant level above the ITTC C_F correlation line at higher Froude Numbers. The large hump is likely to be due to transom stern and wave breaking effects in this speed range, before the transom runs clear, which the wave measurement techniques are unable to capture. Also, the accurate measurement of wave resistance was further hindered in the critical speed region by the presence of solitons which are amplified by the finite width of the tank.

Fig. 26 shows the influence of $L/\nabla^{1/3}$ and, like the deep water results, in the Fn_L range 0.3 to 0.5 there is an increase in resistance with decrease in $L/\nabla^{1/3}$.

The results in Fig. 27 suggest that the effect of hull separation, S/L , is largest in the range of Fn_L 0.3 to 0.5. At higher speeds there is little difference between the two separations, which is similar to the deep water results.

Fig. 28 shows the influence of water depth on resistance. As noted in the earlier resistance diagrams, near the critical depth Froude Numbers there is a distinct rise in resistance due to shallow water effects, this being larger for the smaller 200mm water depth. It is interesting to note that, at the (same) higher length Froude Numbers, the resistance results for both shallow water (supercritical) and deep water (sub-critical) are at a similar level. At the same time their actual wave patterns will be significantly different and this should be taken note of in wave wash investigations.

The results in Fig. 29 compare the resistance for Models 5b and 5s which have distinctly different hull forms. It is noted that the differences due to hull form are very small.

6.2 Running sinkage and trim

The results for running sinkage at the two water depths are shown in Figs. 30 to 37. It is seen that as speed approaches critical Froude Number ($Fn_H = 1.0$) the model rises (negative sinkage), then sinks significantly through the critical speed region before rising again at higher speeds. At the higher supercritical speeds the monohull and catamaran with separation $S/L = 0.4$ are broadly the same as the deep water results, [1-4], whereas the monohull results are lower than the deep water case and the catamaran with separation $S/L = 0.2$ is consistently higher for all models (i.e. change in $L/\nabla^{1/3}$) and both water depths. This would suggest that interference between the catamaran hulls, particularly with narrow separation, is having a

significant effect on running sinkage in shallow water. This might be an important operational consideration if keel to ground clearances become small.

The results for running trim at the two water depths are shown in Figs. 38 to 45. It is seen that in all cases there is a distinct increase in running trim as speed passes through the critical speed region, with the results being a little higher in the 400mm water depth. These increases are significantly higher than those in deep water, [1-4]. At higher supercritical speeds, the running trim for Model 4b is lower than the deep water results, whereas the results for Models 5b, 6b and 5s are similar to the deep water results.

6.3 Wave properties

6.3.1 General

An example of the multiple wave cuts gathered during one test run are shown in Fig. 46. Comprehensive results for all test cases are given in [6, 7]. These wave profiles can be used for various purposes including wave pattern analysis to determine the distribution of wave energy/resistance and wave resistance, and providing information about the waves such as the maximum wave height, distribution of wave energy and direction of propagation of the waves for use in wave wash studies.

6.3.2 Distribution of wave resistance (energy)

The distribution of the wave resistance, or energy, at different speeds is shown in Figs. 48 to 173. The wave pattern analysis considers the wave system to be made up of a discrete set of waves propagating at various angles. When plotted to a base of propagation angle, the distribution of wave energy in the wave system can clearly be seen. In Fig. 48 the vessel is travelling at sub-critical speed and the energy is distributed between the transverse waves, up to about 35° , and divergent waves above 35° . At a supercritical speed such as in Fig. 52, only divergent waves are present. The transverse wave system is unable to travel at a speed greater than $(gh)^{1/2}$ and is consequently left behind. Knowledge of these wave energy distributions is useful in assessing the influence on ship resistance of changes such as hull shape or catamaran hull separation, and the likely concentrations of energy at particular wave propagation angles for wave wash investigations.

7 Conclusions

7.1 The results of the investigation provide a better understanding of the resistance and distribution of wave resistance/ energy of high speed displacement craft in shallow water.

7.2 In all cases the resistance showed a distinct increase near the critical depth Froude Number ($F_{nH}=1.0$). This increase is larger for the smaller water depth, suggesting that this may arise from the smaller under keel clearance.

7.3 At sub-critical and supercritical speeds the resistance is effectively independent of water depth.

7.4 In shallow water, as the speed approaches critical F_{nH} , the vessel firstly rises then sinks significantly through the critical region before rising again at higher speeds. The significant running sinkage might be an important operational consideration if keel to ground clearances become small.

7.5 There is a distinct increase in running trim as the speed passes through the critical speed region. These increases were found to be considerably higher than for deep water.

7.6 The data derived and presented, besides providing a better insight into the performance of high speed monohulls and catamarans in shallow water, are very suitable for design and wave wash applications and for the validation of theoretical analyses.

Acknowledgements

The work described in this report covers part of a research project funded by EPSRC and industry and managed by Marinetech South Ltd.

References

1. Insel, M., "An investigation into the resistance components of high speed displacement catamarans", Ph.D. Thesis, Ship Science, University of Southampton, 1990
2. Insel, M. and A.F. Molland, "An investigation into the resistance components of high speed displacement catamarans". Transactions of the Royal Institution of Naval Architects, 1992. **134**.
3. Molland, A.F., J.F. Wellicome, and P.R. Couser, "Resistance experiments on a systematic series of high speed catamaran forms: Variation of length-displacement ratio and breadth-draught ratio". Transactions of the Royal Institution of Naval Architects, 1996. **138**.
4. Wellicome, J.F., A.F. Molland, J. Cic, and D.J. Taunton, "Resistance experiments on a high speed displacement catamaran of series 64 form". Ship Science Report 106, Department of Ship Science, University of Southampton 1999
5. Molland, A.F., P.A. Wilson, and D.J. Taunton, "A systematic series of experimental wash wave measurements for high speed displacement monohull and catamaran forms in shallow water." Ship Science Report 122, University of Southampton 2002
6. Molland, A.F., P.A. Wilson, and D.J. Taunton, "Further experimental wash wave measurements for high speed displacement catamaran forms in shallow water." Ship Science Report 123, University of Southampton 2002
7. Molland, A.F., P.A. Wilson, and D.J. Taunton, "Experimental measurement of the wash characteristics of a fast displacement catamaran in deep water." Ship Science Report 124, University of Southampton 2002
8. Molland, A.F., P.A. Wilson, and D.J. Taunton, "Theoretical prediction of the characteristics of ship generated near-field wash waves". Ship Science Report 125, University of Southampton 2002
9. Molland, A.F., J.F. Wellicome, and P.R. Couser, "Resistance experiments on a systematic series of high speed displacement catamaran forms: Variation of length-displacement ratio and breadth-draught ratio". Ship Science Report 71, University of Southampton 1994
10. Bailey, D., "The npl high speed round bilge displacement hull series". Maritime Technology Monograph, Royal Institute of Naval Architects, 1976. **4**.
11. Yeh, H.Y.H., "Series 64 resistance experiments on high-speed displacement forms". Marine Technology, 1965. **2(3)**.
12. Dand, I.W., T.A. Dinham-Peren, and L. King. "Hydrodynamic aspects of a fast catamaran operating in shallow water". in *RINA International Conference on the Hydrodynamics of High Speed Craft*. 1999. London.

Tables

Table 1: Principal particulars of models (Demihulls).

	Models			
Model	4b	5b	6b	5s
Length [m]	1.6	1.6	2.1	1.6
$L/\nabla^{1/3}$	7.4	8.5	9.5	8.5
L/B	9.0	11.0	13.1	12.8
B/T	2.0	2.0	2.0	2.0
C_B	0.397	0.397	0.397	0.537
C_P	0.693	0.693	0.693	0.633
C_M	0.565	0.565	0.565	0.848
WSA [m ²]	0.338	0.276	0.401	0.261
LCB [%]	-6.4	-6.4	-6.4	-6.4

Table 2: Residuary resistance coefficients (C_R) x1000 for Model 4b. [Model length =1.6m]

Fn	Deep			H=400mm			H=200mm		
	Monohull	S/L=0.2	S/L=0.4	Monohull	S/L=0.2	S/L=0.4	Monohull	S/L=0.2	S/L=0.4
0.25	2.629	3.686	3.365	3.657	4.007	3.045	3.932	4.801	6.455
0.30	3.532	4.311	4.150	5.887	4.664	4.394	13.709	13.841	18.134
0.35	3.763	5.483	4.557	7.886	5.849	6.832	13.835	19.577	19.413
0.40	4.520	5.897	5.940	8.975	10.891	10.549	10.579	13.878	14.292
0.45	5.402	7.748	7.078	9.449	15.658	12.894	7.504	8.368	10.360
0.50	5.389	8.420	6.922	6.606	12.187	8.474	5.444	4.592	7.560
0.55	4.865	8.099	6.145	5.108	9.482	6.316	4.675	3.943	6.138
0.60	4.276	7.159	5.315	4.385	7.482	5.238	4.126	3.502	4.944
0.65	3.787	6.008	4.605	3.876	5.835	4.473	3.709	3.215	3.978
0.70	3.394	4.769	4.098	3.520	4.591	3.945	3.390	3.002	3.248
0.75	3.098	4.041	3.718	3.259	3.793	3.586	3.141	2.853	2.781
0.80	2.848	3.605	3.440	3.036	3.458	3.322	2.931	2.737	2.582
0.85	2.647	2.647	3.247	2.823	3.318	3.093	2.737	2.634	2.490
0.90	2.476	2.476	3.078	2.636	3.197	2.899	2.565	2.546	2.412
0.95	2.361	2.361	2.968	2.494	3.113	2.756	2.432	2.481	2.358
1.00	2.347	2.347	2.882	2.415	3.070	2.681	2.350	2.448	2.331

Table 3: Residuary resistance coefficients (C_R) x1000 for Model 5b. [Model length =1.6m]

Fn	Deep			H=400mm			H=200mm		
	Monohull	S/L=0.2	S/L=0.4	Monohull	S/L=0.2	S/L=0.4	Monohull	S/L=0.2	S/L=0.4
0.25	2.362	2.843	3.26	2.782	3.248	3.165	3.081	5.539	3.847
0.3	2.632	3.643	3.693	3.072	5.995	5.200	4.510	11.898	10.579
0.35	2.890	4.194	3.711	3.656	8.030	6.754	10.056	12.755	12.398
0.4	3.514	4.520	4.622	4.469	9.049	7.519	5.451	8.702	7.125
0.45	3.691	5.506	4.960	5.616	9.189	7.763	4.045	6.122	3.910
0.5	3.518	5.581	4.632	4.145	6.371	4.922	3.460	4.381	2.944
0.55	3.125	4.927	4.057	3.039	4.812	3.724	3.110	3.614	2.629
0.6	2.851	4.177	3.504	2.754	3.859	3.221	2.825	3.010	2.410
0.65	2.599	3.555	3.090	2.508	3.142	2.877	2.599	2.535	2.260
0.7	2.285	3.051	2.759	2.312	2.639	2.648	2.420	2.182	2.150
0.75	2.155	2.744	2.515	2.167	2.330	2.491	2.279	1.954	2.068
0.8	2.010	2.529	2.327	2.057	2.186	2.362	2.166	1.845	2.000
0.85	1.938	2.383	2.163	1.959	2.103	2.242	2.063	1.790	1.935
0.9	1.830	2.298	2.111	1.873	2.035	2.140	1.973	1.743	1.879
0.95	1.852	2.221	2.128	1.809	1.988	2.065	1.904	1.710	1.835
1	1.803	2.186	2.145	1.775	1.964	2.025	1.863	1.693	1.812

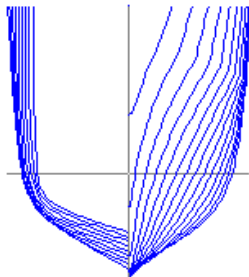
Table 4: Residuary resistance coefficients (C_R) x1000 for Model 6b.
[Model length = 1.6m deep, 2.1m shallow]

Fn	Deep			H=400mm			H=200mm		
	Monohull	S/L=0.2	S/L=0.4	Monohull	S/L=0.2	S/L=0.4	Monohull	S/L=0.2	S/L=0.4
0.25	2.136	3.217	3.203	2.583	3.174	2.985	4.870	3.146	8.788
0.30	2.255	3.769	3.251	2.598	4.189	4.909	7.851	3.916	12.365
0.35	2.150	3.667	3.502	2.723	5.556	6.126	5.867	4.994	6.977
0.40	2.639	4.007	3.913	2.874	7.456	7.035	3.805	6.210	4.395
0.45	2.696	4.534	3.950	3.064	5.530	4.221	2.611	7.466	3.460
0.50	2.510	4.379	3.592	2.897	4.276	3.074	2.283	5.430	3.142
0.55	2.338	3.734	3.196	2.499	3.426	2.396	2.027	4.422	2.888
0.60	2.084	3.144	2.866	2.041	2.836	1.943	1.845	3.666	2.711
0.65	1.900	2.738	2.635	1.686	2.451	1.681	1.720	3.111	2.611
0.70	1.747	2.477	2.468	1.580	2.225	1.569	1.633	2.701	2.586
0.75	1.656	2.311	2.339	1.588	2.088	1.529	1.563	2.417	2.587
0.80	1.575	2.184	2.241	1.600	2.110	1.490	1.504	2.237	2.587
0.85	1.527	2.093	2.172	1.628	2.406	1.452	1.466	2.113	2.587
0.90				1.673	3.088	1.420	1.454	2.073	2.587
0.95				1.339	4.264	1.611	1.477	2.185	2.587
1.00				0.040	6.046	2.352	1.540	2.507	2.587

Table 5: Residuary resistance coefficients (C_R) x1000 for Model 5s. [Model length =1.6m]

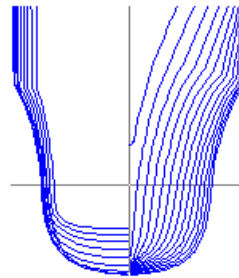
Fn	Deep			H=400mm			H=200mm		
	Monohull	S/L=0.2	S/L=0.4	Monohull	S/L=0.2	S/L=0.4	Monohull	S/L=0.2	S/L=0.4
0.25	2.450	3.133	2.720	1.888	1.510	2.313	3.329	4.773	3.914
0.30	2.794	3.388	3.177	2.312	1.939	2.827	9.752	12.598	12.207
0.35	2.769	3.501	3.281	2.615	2.519	3.240	10.238	13.944	13.316
0.40	3.469	4.911	4.585	2.815	3.201	3.549	7.205	10.059	7.599
0.45	3.699	6.000	4.918	2.946	4.253	3.727	4.910	6.806	3.976
0.50	3.627	5.843	4.602	2.998	5.145	3.798	3.448	4.578	2.815
0.55	3.379	5.025	4.037	2.941	4.627	3.680	3.011	3.770	2.529
0.60	3.028	4.184	3.571	2.737	3.419	3.264	2.690	3.148	2.337
0.65	2.751	3.543	3.197	2.452	2.679	2.694	2.454	2.673	2.210
0.70	2.461	3.103	2.924	2.153	2.041	2.111	2.282	2.322	2.118
0.75	2.289	2.790	2.715	1.906	1.578	1.662	2.162	2.095	2.049
0.80	2.139	2.650	2.562	1.768	1.366	1.462	2.081	1.982	1.986
0.85	2.056	2.474	2.457	1.677	1.268	1.371	2.017	1.916	1.925
0.90	1.992	2.414	2.382	1.595	1.186	1.289	1.963	1.862	1.871
0.95	1.965	2.320	2.313	1.534	1.130	1.232	1.923	1.823	1.829
1.00	1.917	2.223	2.252	1.502	1.102	1.203	1.902	1.803	1.804

Figures



NPL

Figure 1a: Hull Bodyplans



Series 64

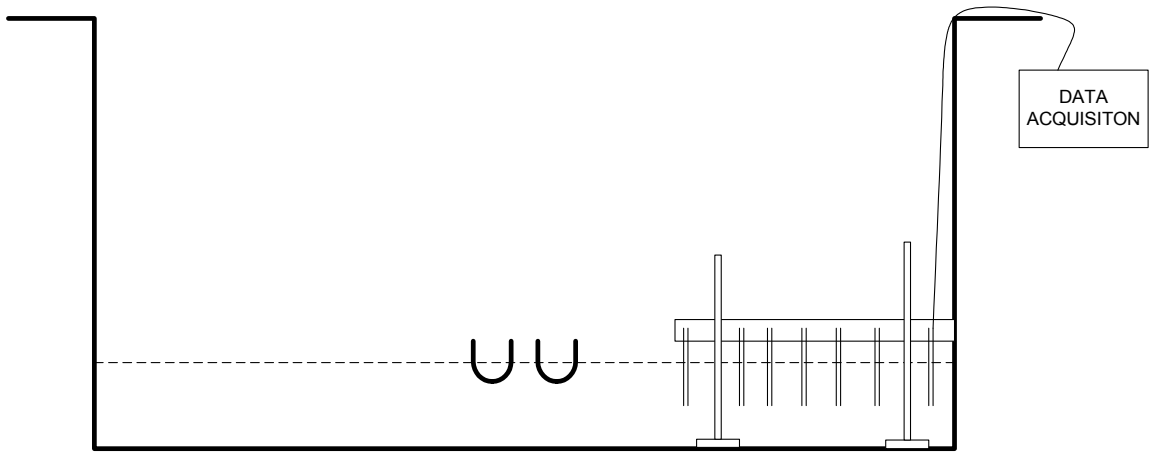


Figure 1b: Schematic of GKN-Westland tank (cross Section)



Figure 1c: View of model passing probe array from beach.

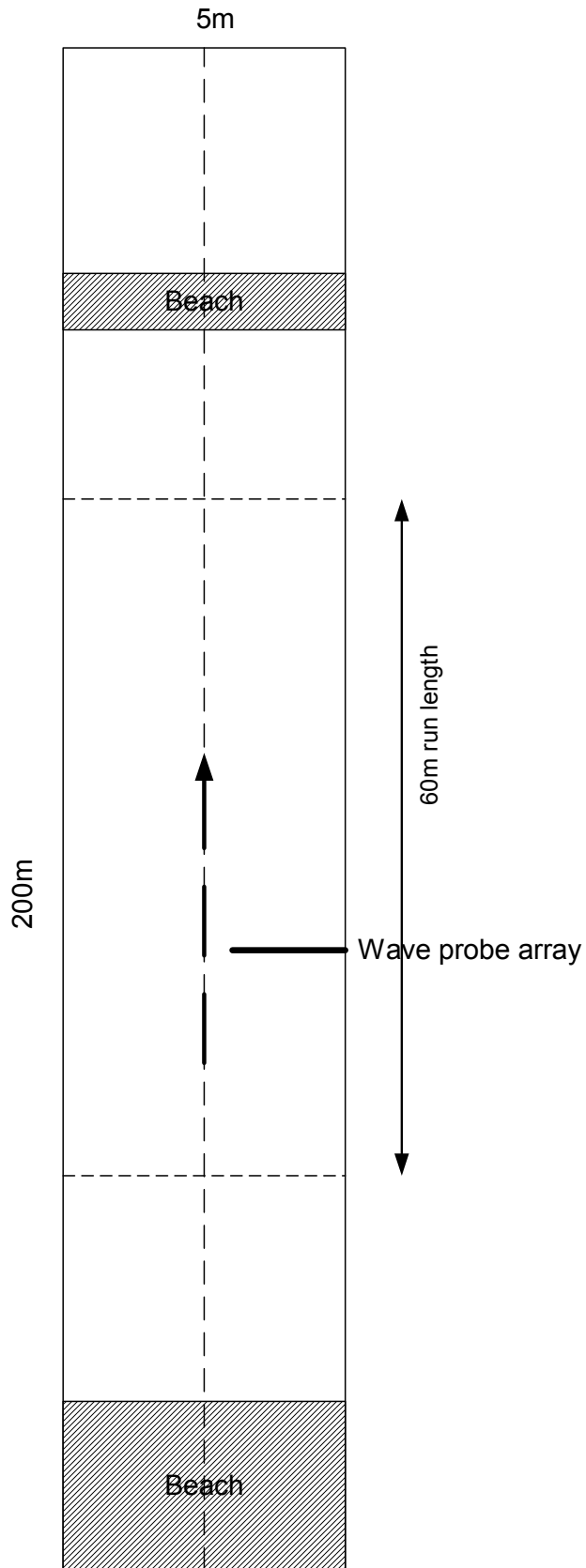


Figure 1d: Schematic of GKN test tank

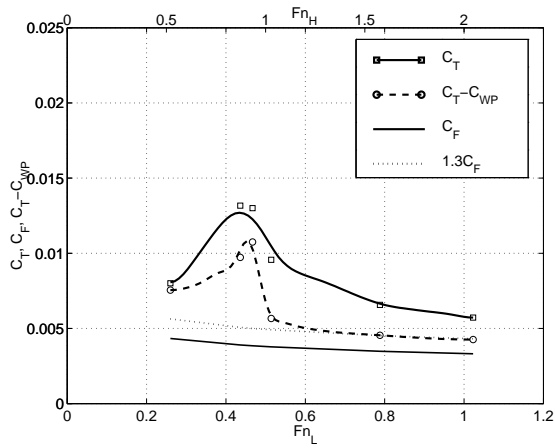


Figure 2: Model 4b, monohull, H=400mm

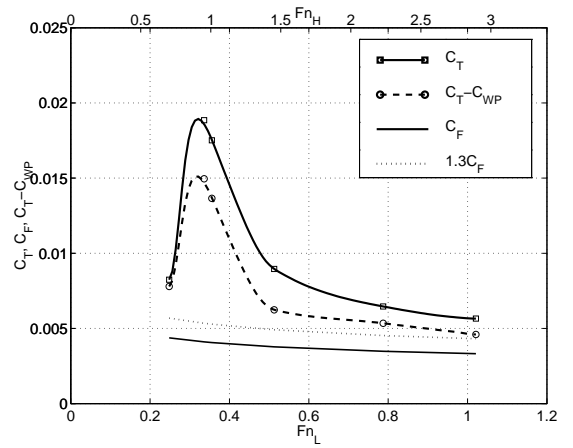


Figure 3: Model 4b, monohull, H=200mm

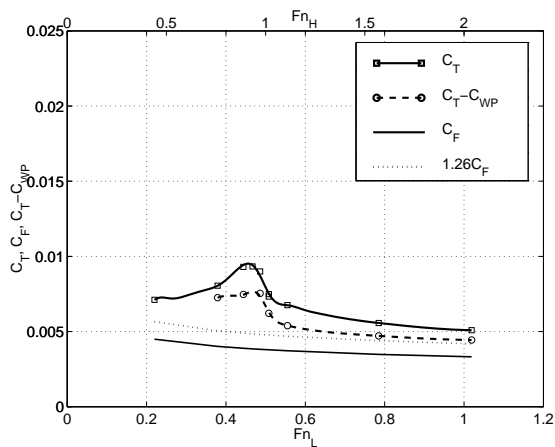


Figure 4: Model 5b, monohull, H=400mm

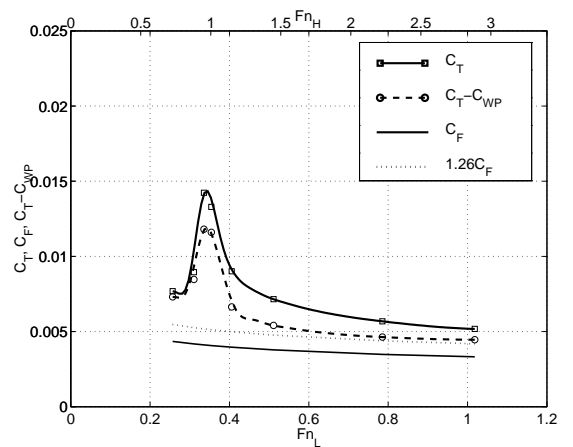


Figure 5: Model 5b, monohull, H=200mm

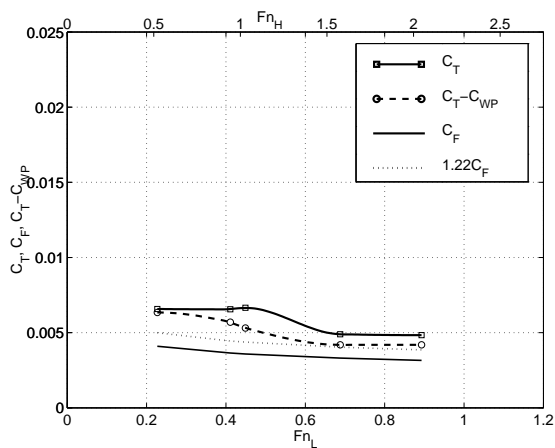


Figure 6: Model 6b, monohull, H=400mm

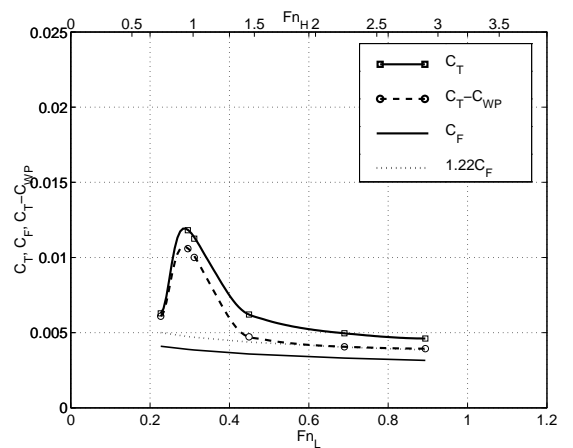


Figure 7: Model 6b, monohull, H=200mm

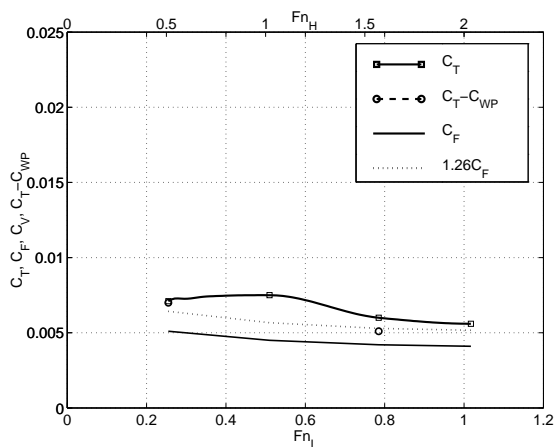


Figure 8: Model 5s, monohull, H=400mm

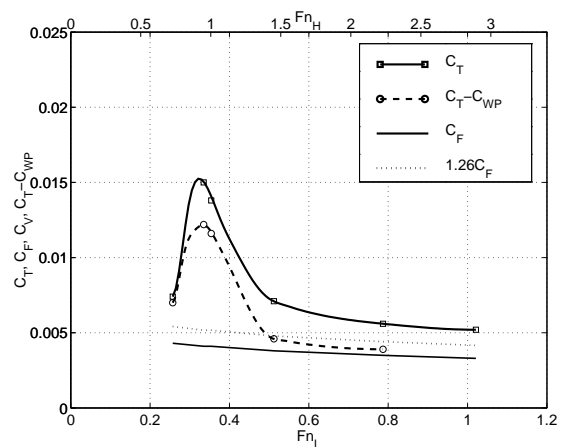


Figure 9: Model 5s, monohull, H=200mm

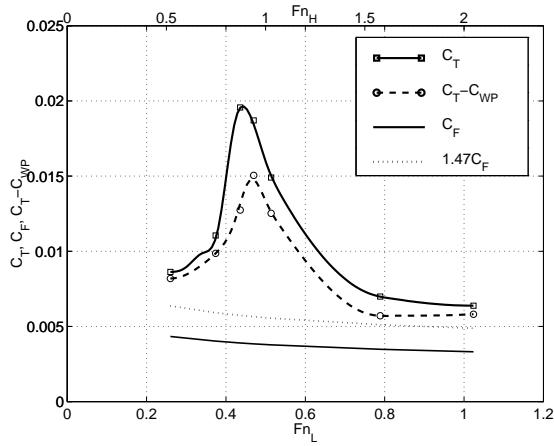


Figure 10: Model 4b, catamaran $S/L=0.2$, $H=400\text{mm}$

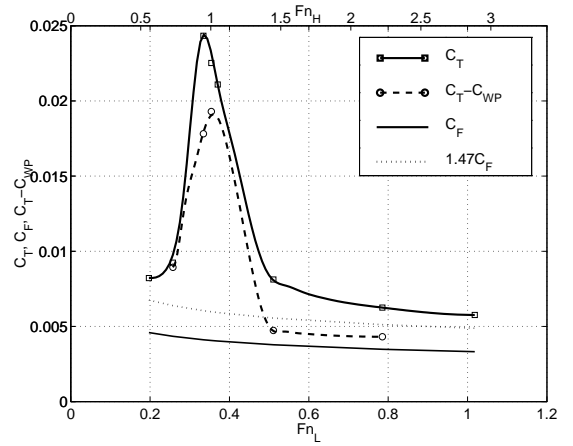


Figure 11: Model 4b, catamaran $S/L=0.2$, $H=200\text{mm}$

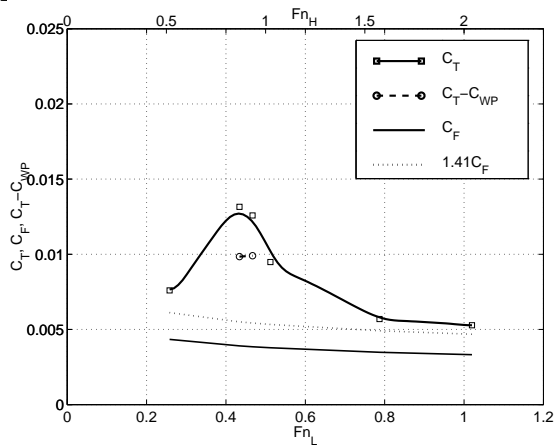


Figure 12: Model 5b, catamaran $S/L=0.2$, $H=400\text{mm}$

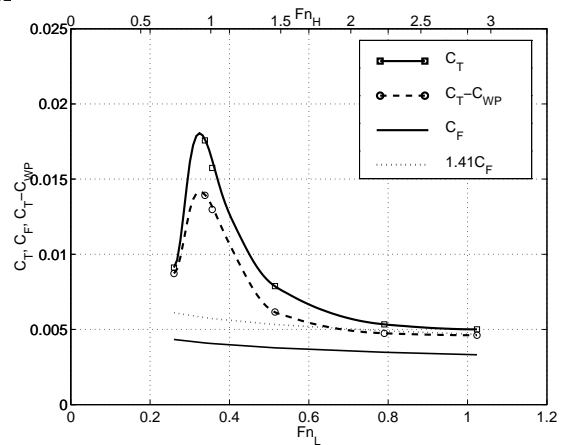


Figure 13: Model 5b, catamaran $S/L=0.2$, $H=200\text{mm}$

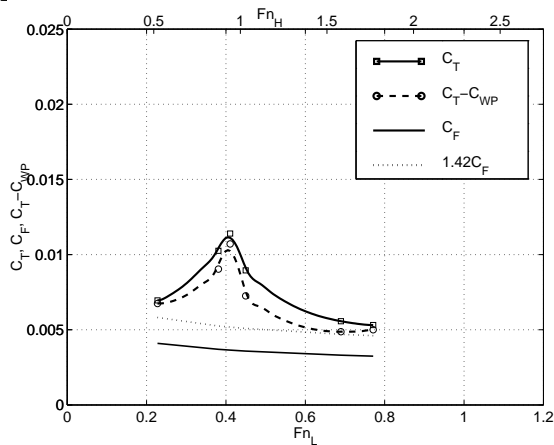


Figure 14: Model 6b, catamaran $S/L=0.2$, $H=400\text{mm}$

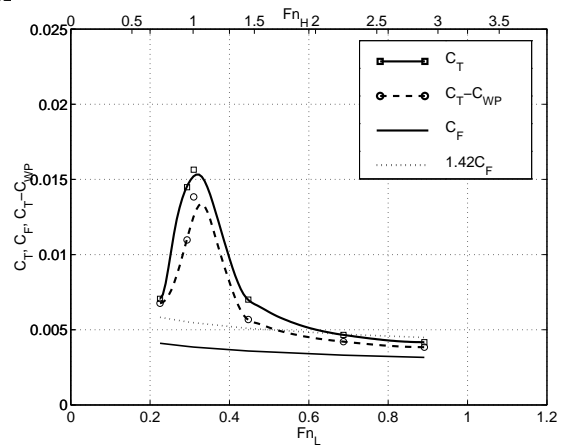


Figure 15: Model 6b, catamaran $S/L=0.2$, $H=200\text{mm}$

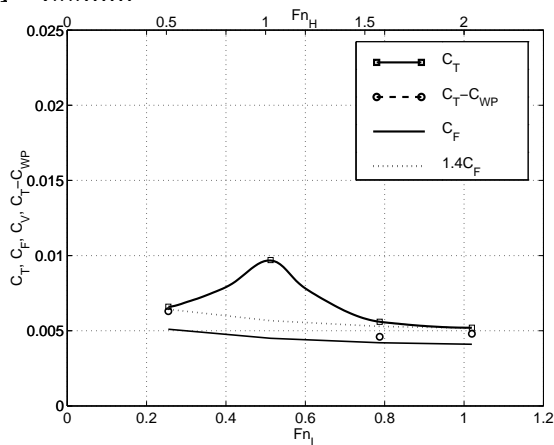


Figure 16: Model 5s, catamaran $S/L=0.2$, $H=400\text{mm}$

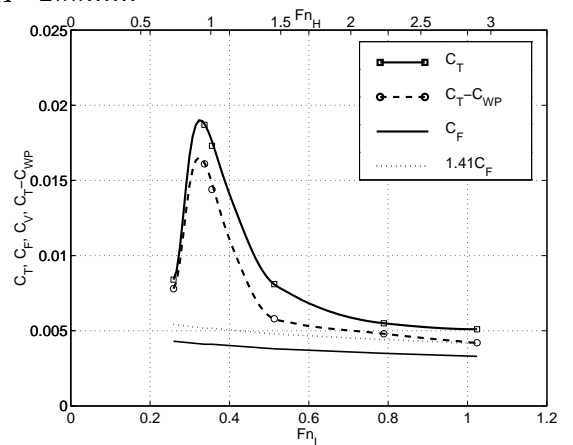


Figure 17: Model 5s, catamaran $S/L=0.2$, $H=200\text{mm}$

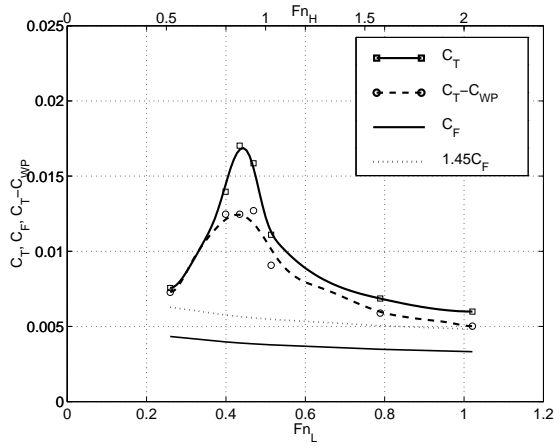


Figure 18: Model 4b, catamaran $S/L=0.4$, $H=400\text{mm}$

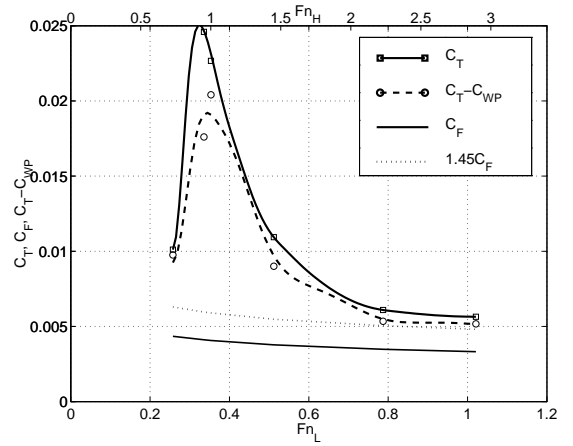


Figure 19: Model 4b, catamaran $S/L=0.4$, $H=200\text{mm}$

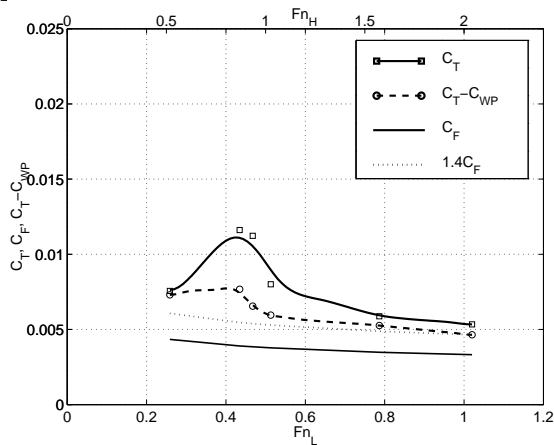


Figure 20: Model 5b, catamaran $S/L=0.4$, $H=400\text{mm}$

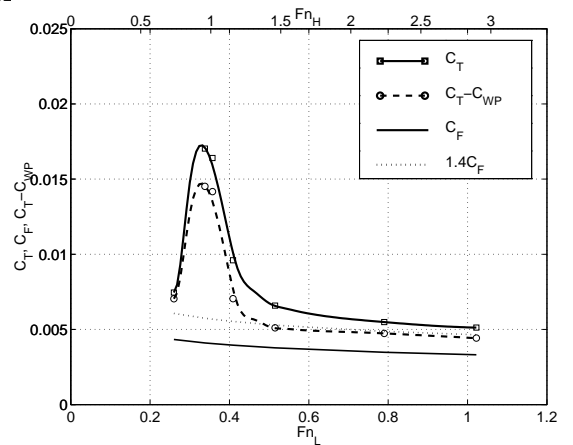


Figure 21: Model 5b, catamaran $S/L=0.4$, $H=200\text{mm}$

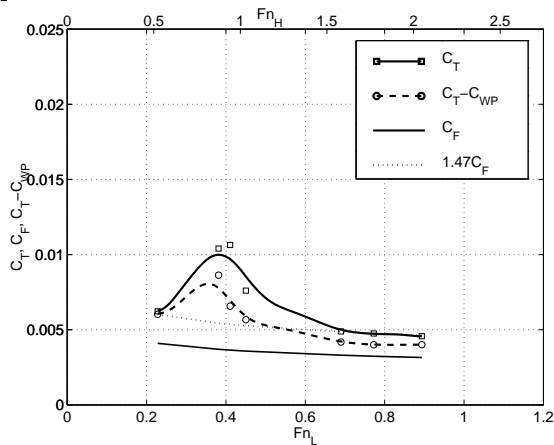


Figure 22: Model 6b, catamaran $S/L=0.4$, $H=400\text{mm}$

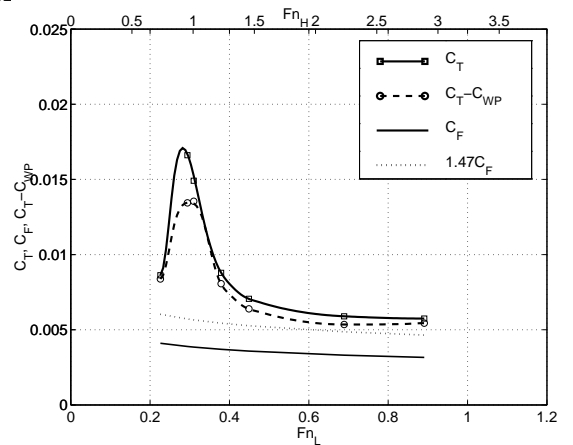


Figure 23: Model 6b, catamaran $S/L=0.4$, $H=200\text{mm}$

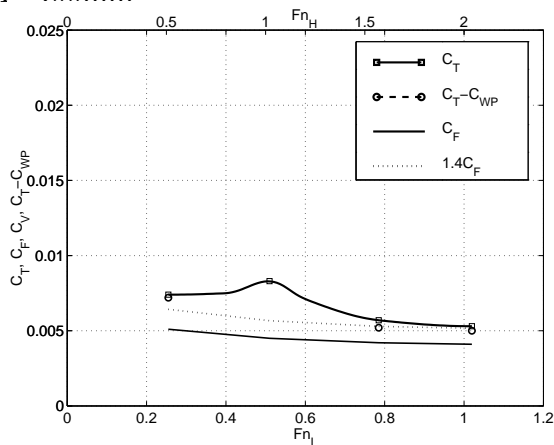


Figure 24: Model 5s, catamaran $S/L=0.4$, $H=400\text{mm}$

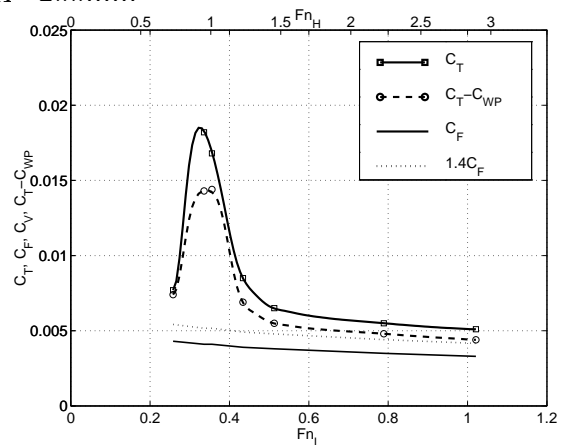


Figure 25: Model 5s, catamaran $S/L=0.4$, $H=200\text{mm}$

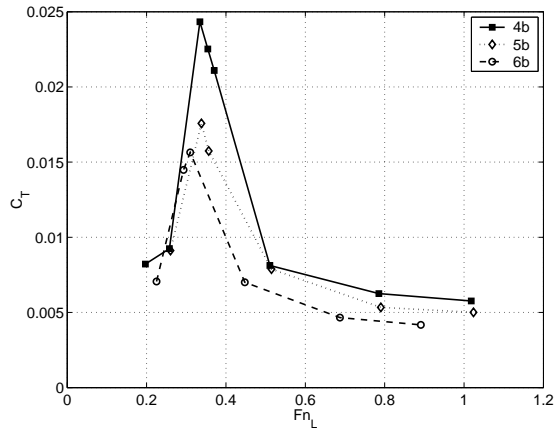


Figure 26: Influence of $L/\nabla^{1/3}$ on C_T , $H=200\text{mm}$, $S/L=0.2$

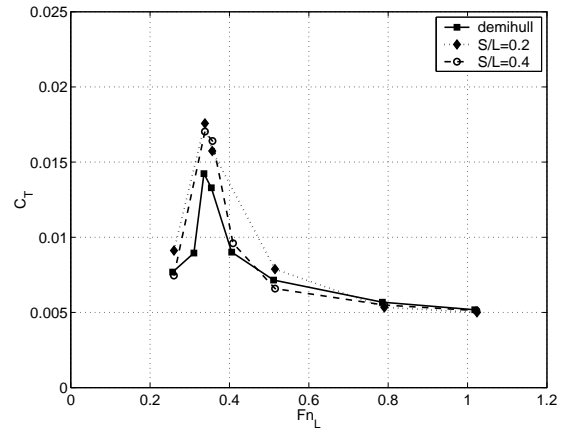


Figure 27: Influence of S/L on C_T , $H=200\text{mm}$, Model 5b

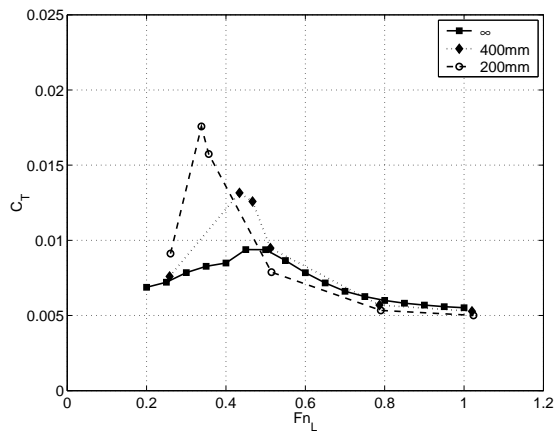


Figure 28: Influence of depth on C_T , Model 5b, $S/L=0.2$

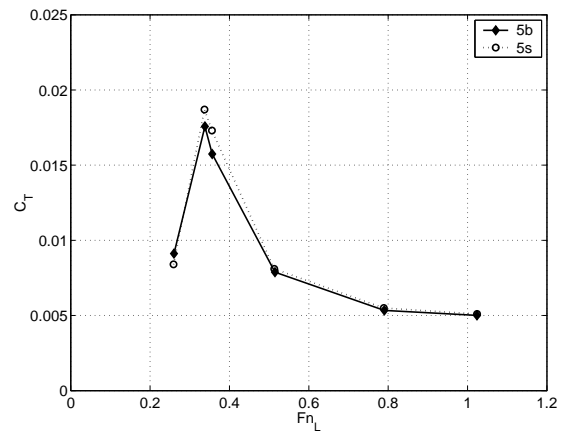


Figure 29: Influence of hull shape on C_T

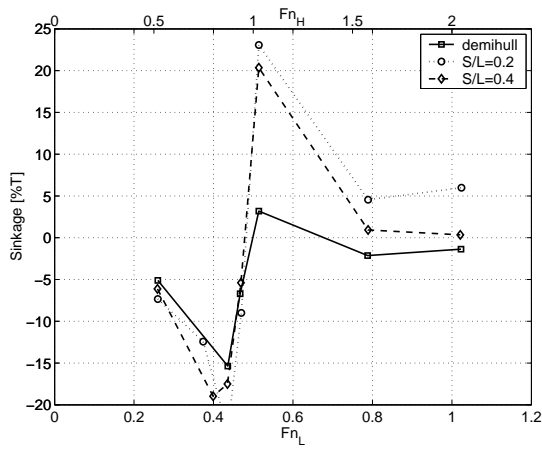


Figure 30: Running sinkage: Model 4b, H=400mm

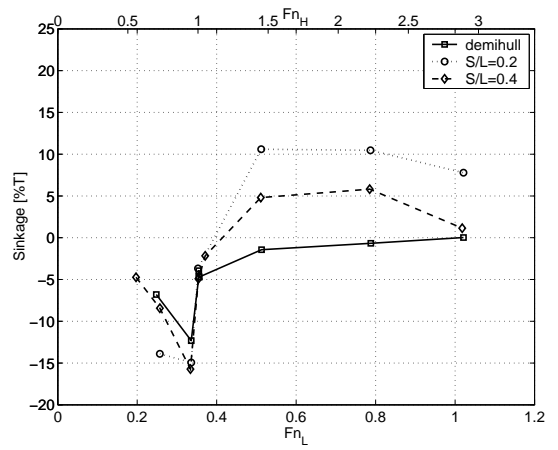


Figure 31: Running sinkage: Model 4b, H=200mm

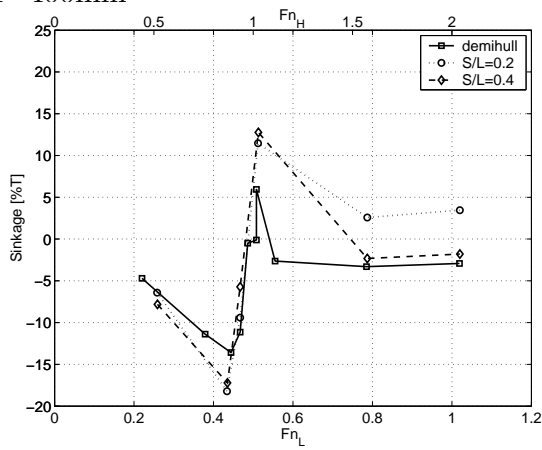


Figure 32: Running sinkage: Model 5b, H=400mm

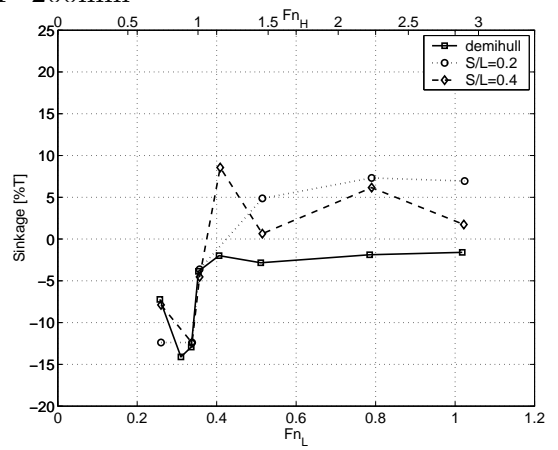


Figure 33: Running sinkage: Model 5b, H=200mm

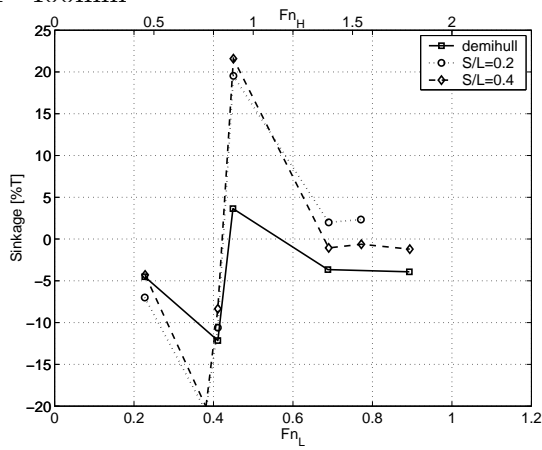


Figure 34: Running sinkage: Model 6b, H=400mm

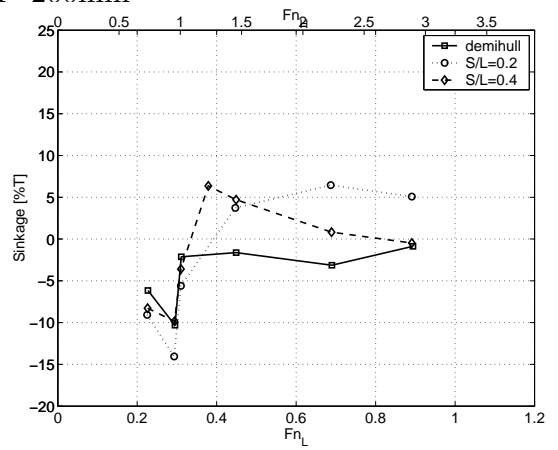


Figure 35: Running sinkage: Model 6b, H=200mm

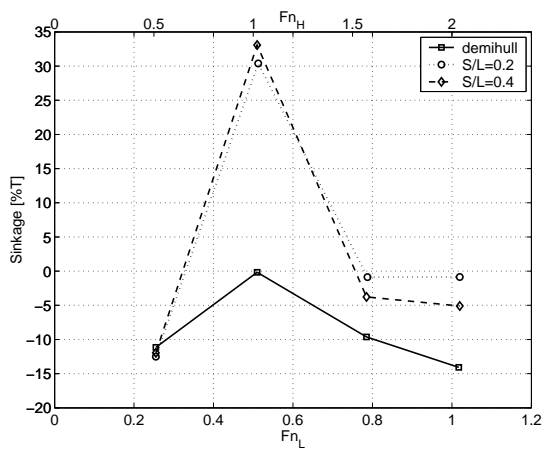


Figure 36: Running sinkage: Model 5s, H=400mm

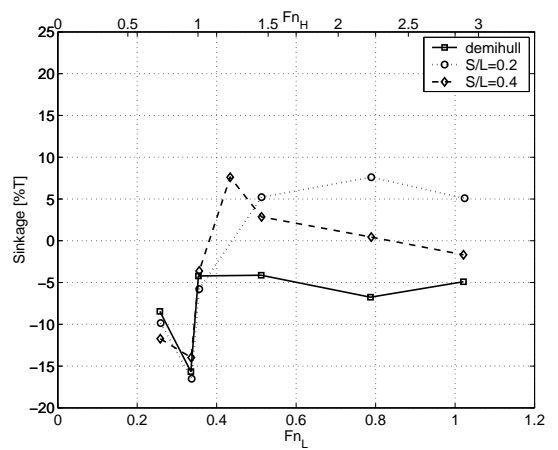


Figure 37: Running sinkage: Model 5s, H=200mm

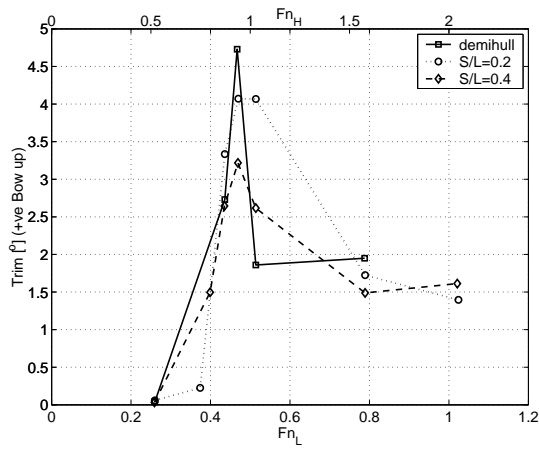


Figure 38: Running trim: Model 4b, H=400mm

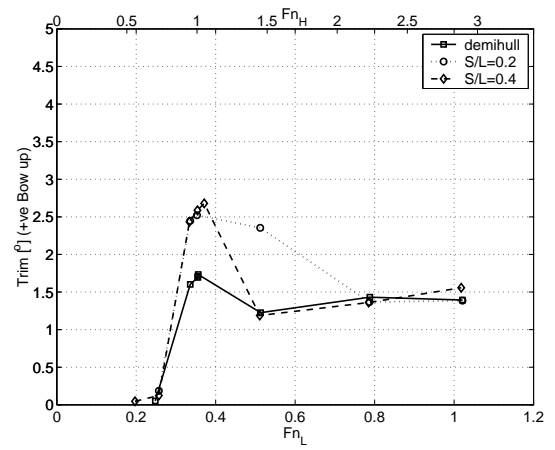


Figure 39: Running trim: Model 4b, H=200mm

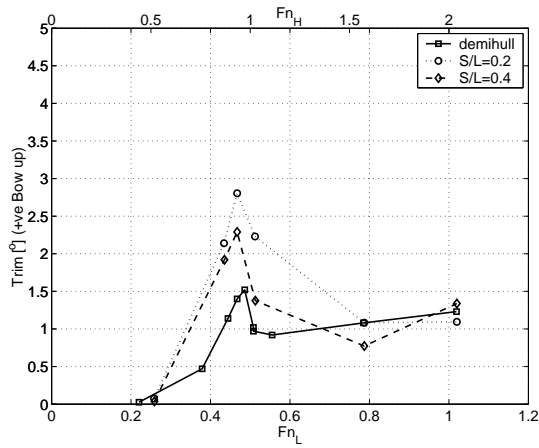


Figure 40: Running trim: Model 5b, H=400mm

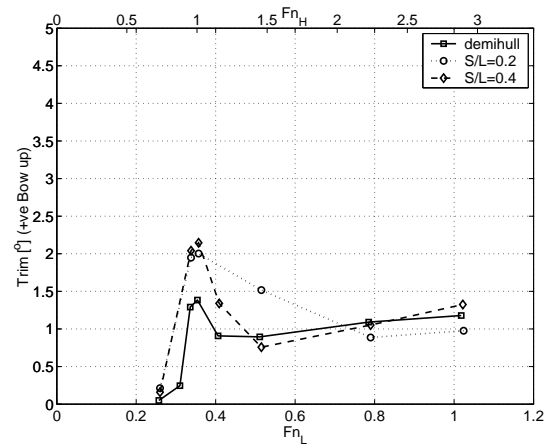


Figure 41: Running trim: Model 5b, H=200mm

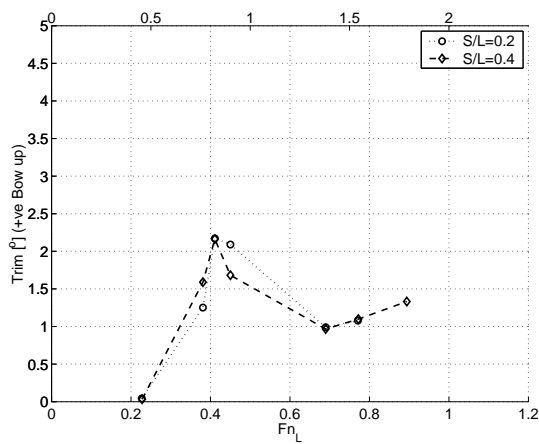


Figure 42: Running trim: Model 6b, H=400mm

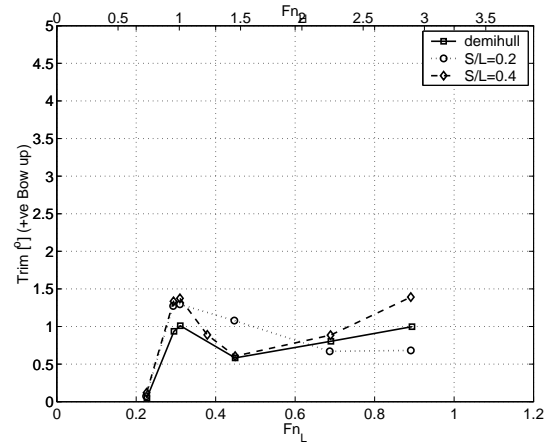


Figure 43: Running trim: Model 6b, H=200mm

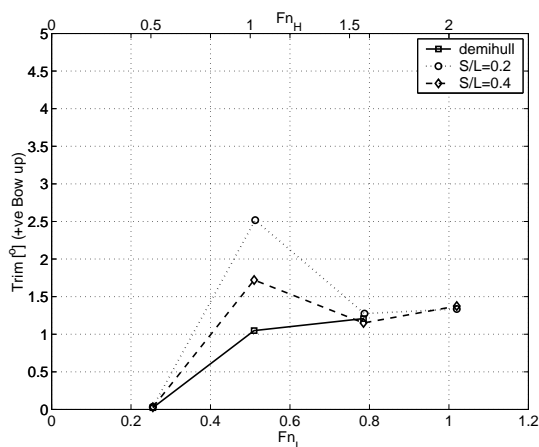


Figure 44: Running trim: Model 5s, H=400mm

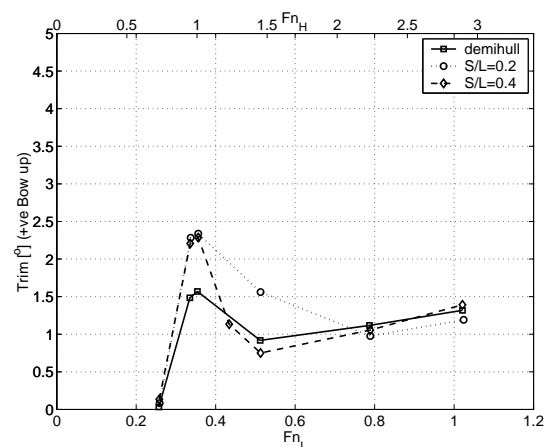


Figure 45: Running trim: Model 5s, H=200mm

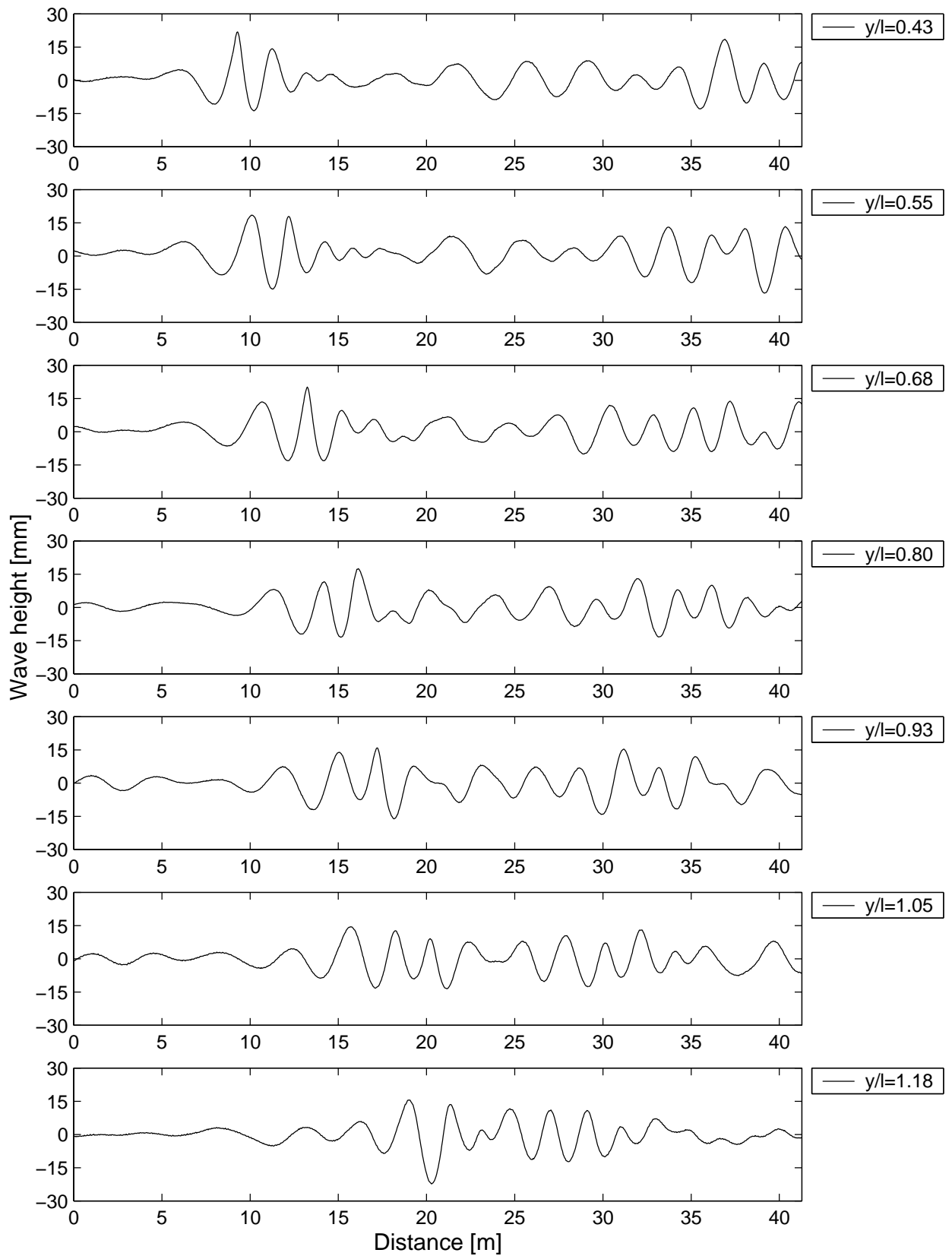


Figure 46: Example wave cuts: Model 5b demihull, $H=400\text{mm}$, $V=4.0\text{ m/s}$, $Fn_L = 1.0$, $Fn_H = 2.0$

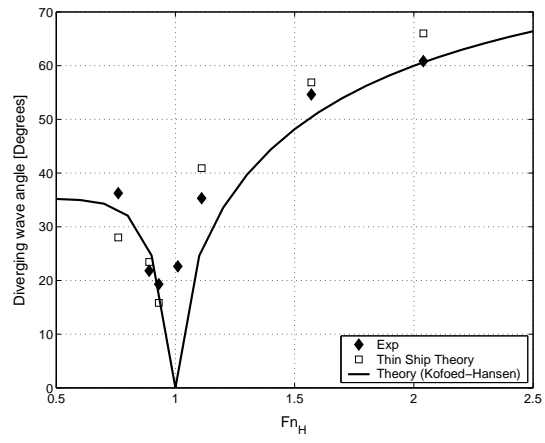


Figure 47: Diverging wave angle with depth Froude number: Model 5s $S/L=0.2$, $H=200\text{mm}$.

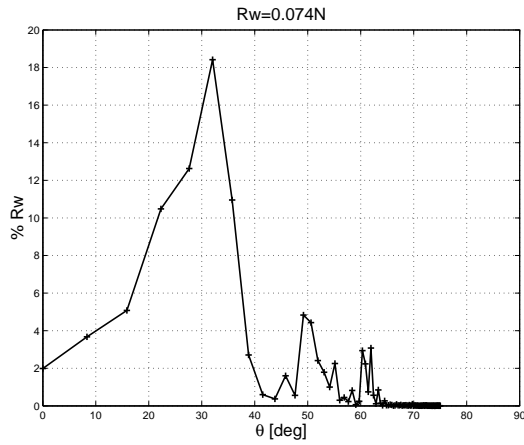


Figure 48: Model 4b: mono, $V=1\text{m/s}$
 $H=400\text{mm}$

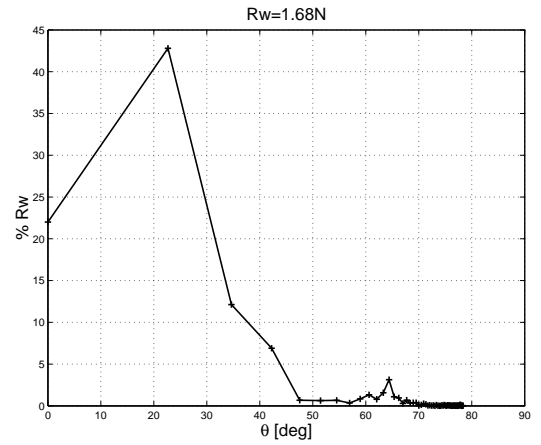


Figure 49: Model 4b: mono, $V=1.7\text{m/s}$
 $H=400\text{mm}$

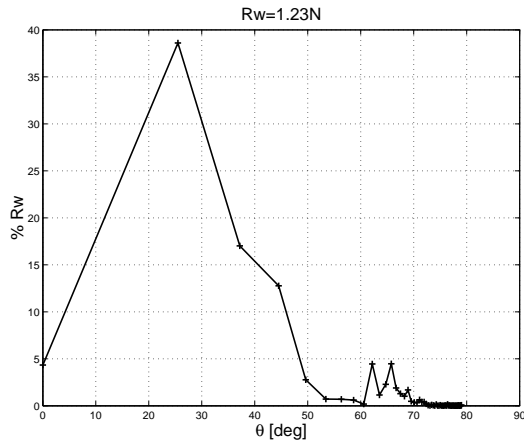


Figure 50: Model 4b: mono, $V=1.8\text{m/s}$
 $H=400\text{mm}$

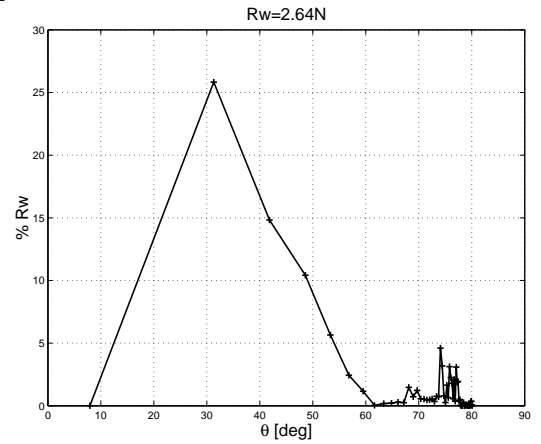


Figure 51: Model 4b: mono, $V=2\text{m/s}$
 $H=400\text{mm}$

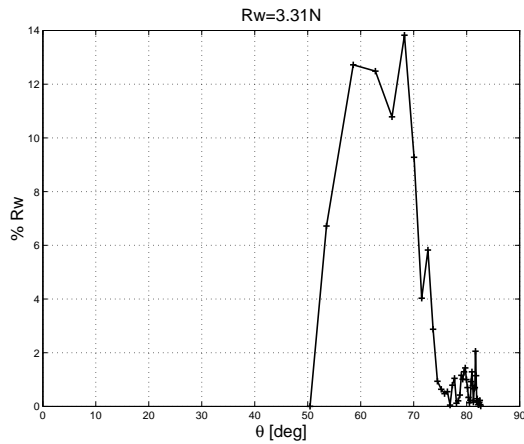


Figure 52: Model 4b: mono, $V=3\text{m/s}$
 $H=400\text{mm}$

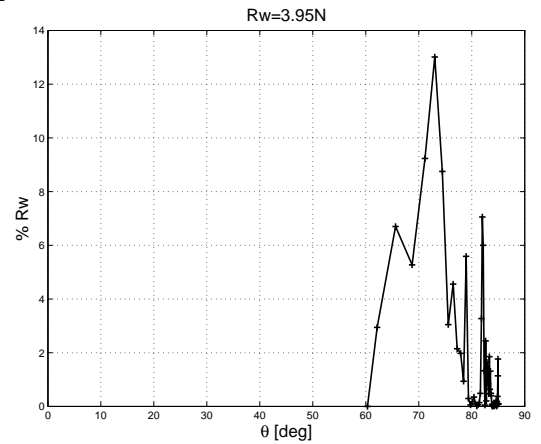


Figure 53: Model 4b: mono, $V=4\text{m/s}$
 $H=400\text{mm}$

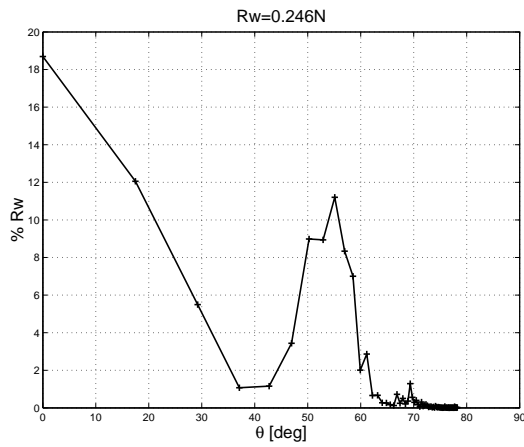


Figure 54: Model 5b: mono, $V=1.5\text{m/s}$
 $H=400\text{mm}$

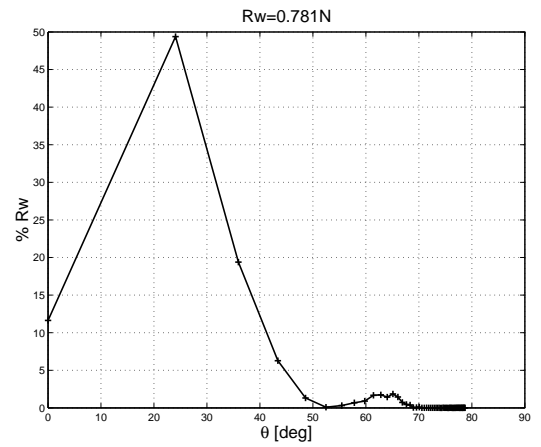


Figure 55: Model 5b: mono, $V=1.7\text{m/s}$
 $H=400\text{mm}$

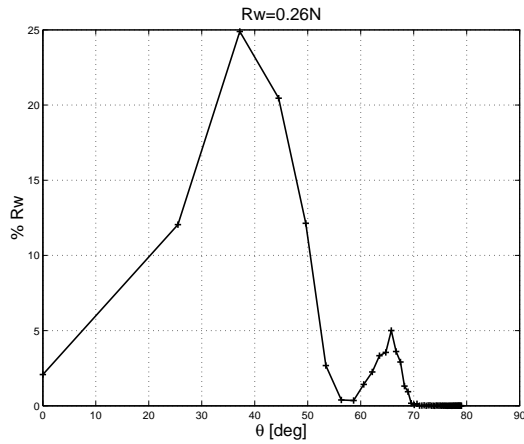


Figure 56: Model 5b: mono, $V=1.8\text{m/s}$
 $H=400\text{mm}$

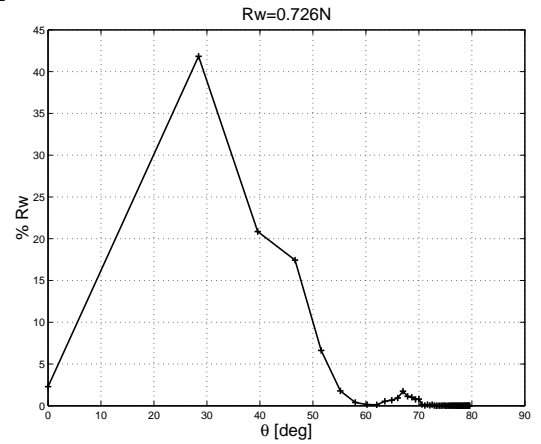


Figure 57: Model 5b: mono, $V=1.9\text{m/s}$
 $H=400\text{mm}$

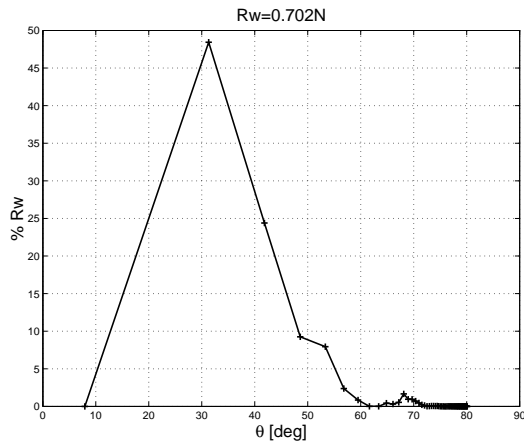


Figure 58: Model 5b: mono, $V=2\text{m/s}$
 $H=400\text{mm}$

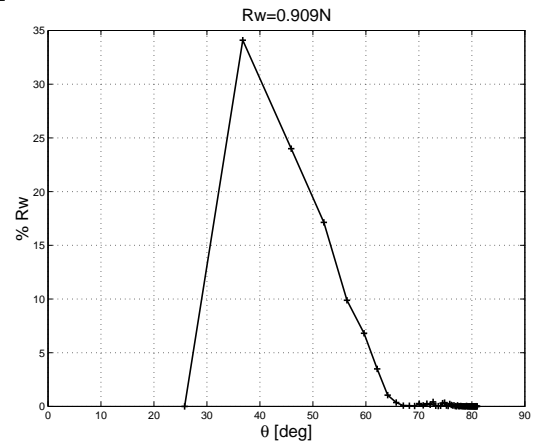


Figure 59: Model 5b: mono, $V=2.2\text{m/s}$
 $H=400\text{mm}$

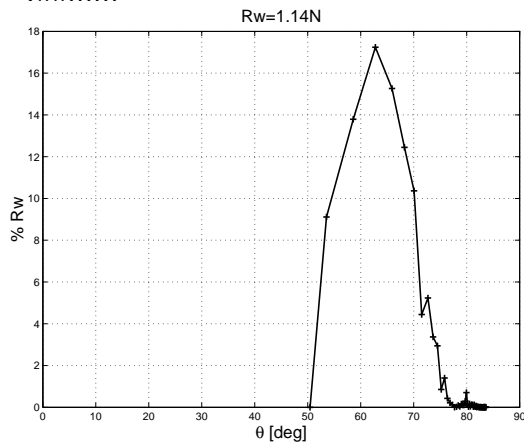


Figure 60: Model 5b: mono, $V=3\text{m/s}$
 $H=400\text{mm}$

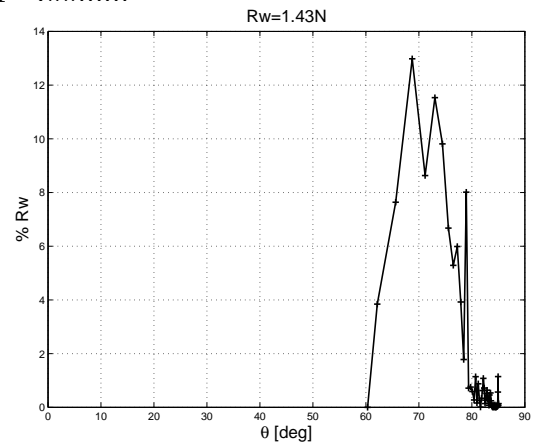


Figure 61: Model 5b: mono, $V=4\text{m/s}$
 $H=400\text{mm}$

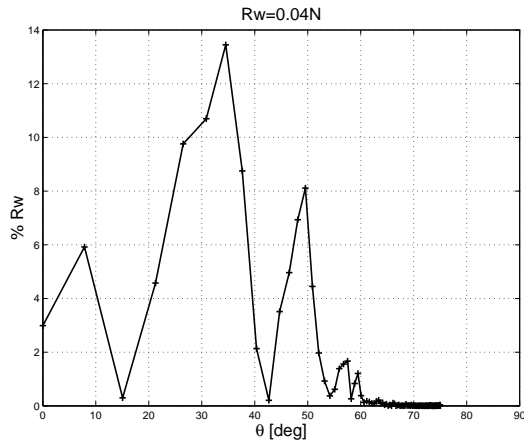


Figure 62: Model 6b: mono, $V=1\text{m/s}$
 $H=400\text{mm}$

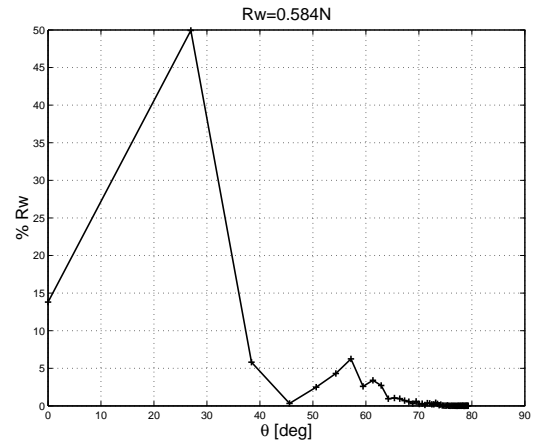


Figure 63: Model 6b: mono, $V=1.8\text{m/s}$
 $H=400\text{mm}$

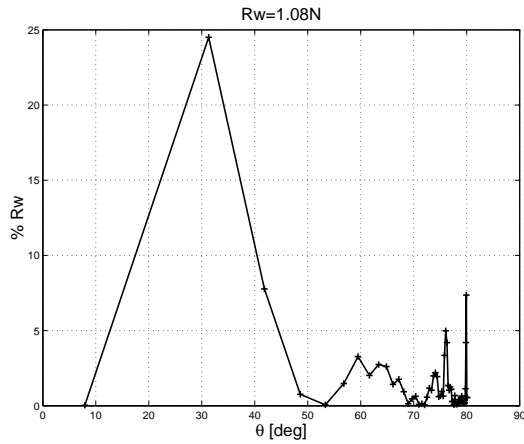


Figure 64: Model 6b: mono, $V=2\text{m/s}$
 $H=400\text{mm}$

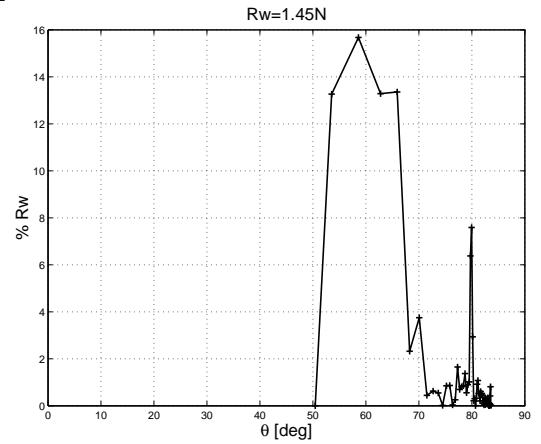


Figure 65: Model 6b: mono, $V=3\text{m/s}$
 $H=400\text{mm}$

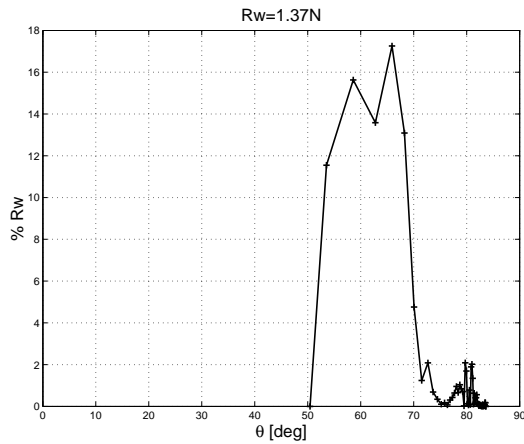


Figure 66: Model 6b: mono, $V=3\text{m/s}$
 $H=400\text{mm}$

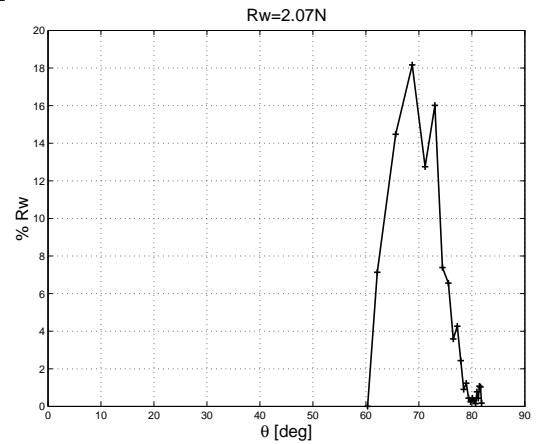


Figure 67: Model 6b: mono, $V=4\text{m/s}$
 $H=400\text{mm}$

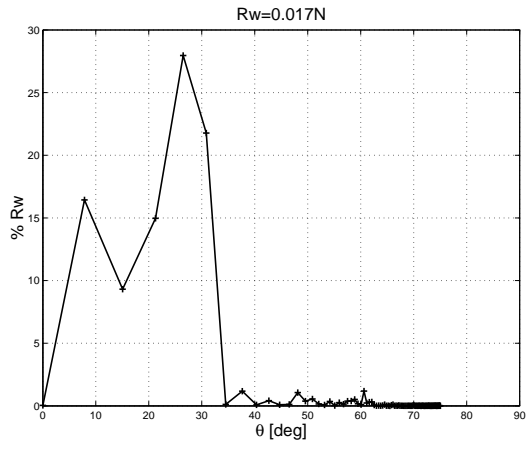


Figure 68: Model 5s: mono, $V=1\text{m/s}$
 $H=400\text{mm}$

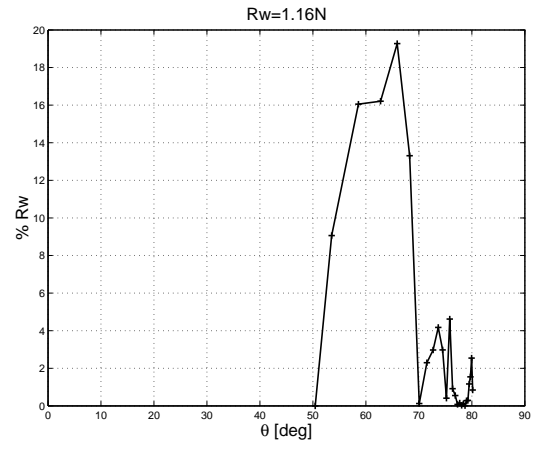


Figure 69: Model 5s: mono, $V=3\text{m/s}$
 $H=400\text{mm}$

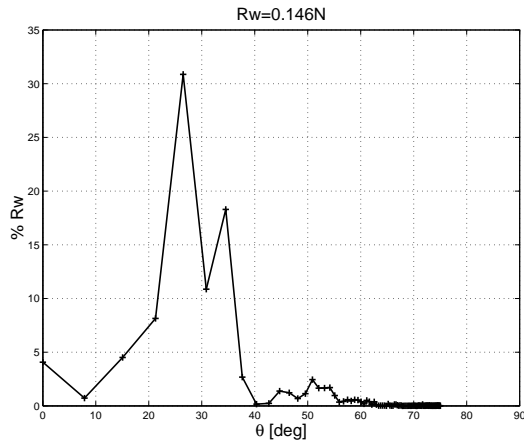


Figure 70: Model 4b: cat $S/L=0.2$, $V=1\text{m/s}$
 $H=400\text{mm}$

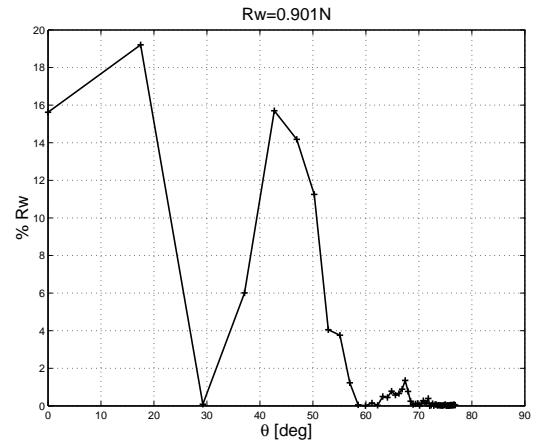


Figure 71: Model 4b: cat $S/L=0.2$,
 $V=1.5\text{m/s}$ $H=400\text{mm}$

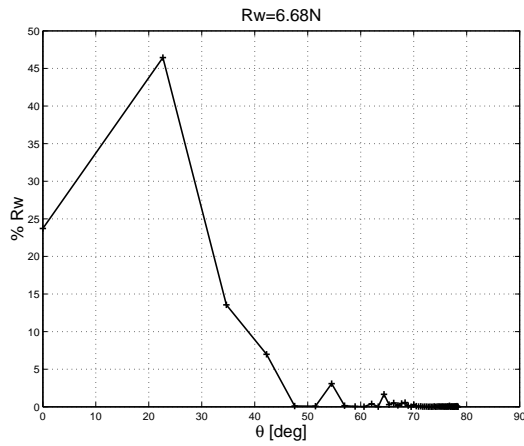


Figure 72: Model 4b: cat $S/L=0.2$,
 $V=1.7\text{m/s}$ $H=400\text{mm}$

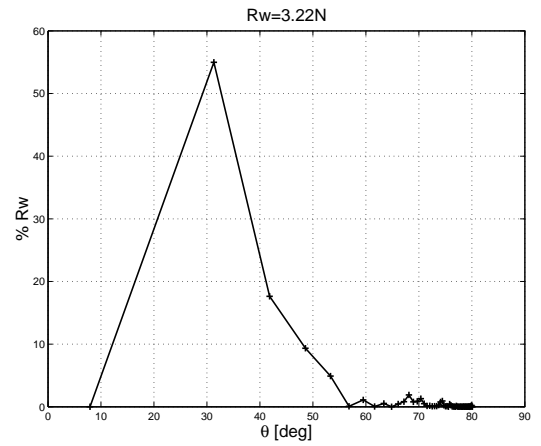


Figure 73: Model 4b: cat $S/L=0.2$, $V=2\text{m/s}$
 $H=400\text{mm}$

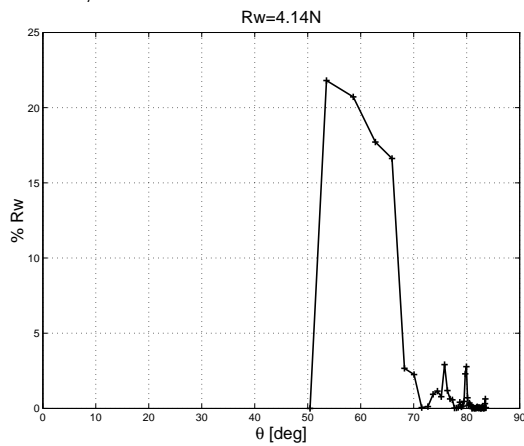


Figure 74: Model 4b: cat $S/L=0.2$, $V=3\text{m/s}$
 $H=400\text{mm}$

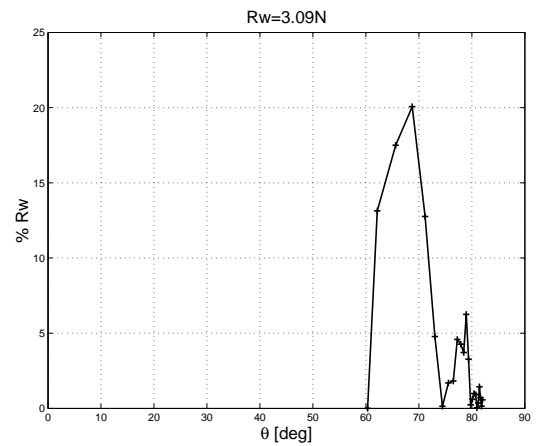


Figure 75: Model 4b: cat $S/L=0.2$, $V=4\text{m/s}$
 $H=400\text{mm}$

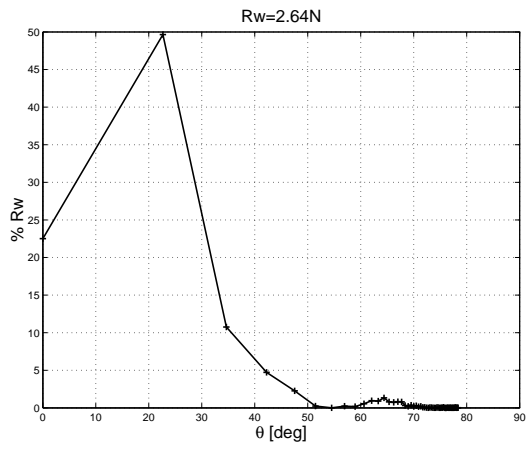


Figure 76: Model 5b: cat S/L=0.2, V=1.7m/s H=400mm

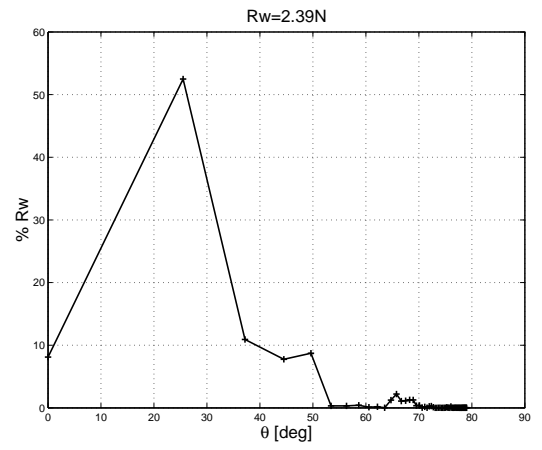


Figure 77: Model 5b: cat S/L=0.2, V=1.8m/s H=400mm

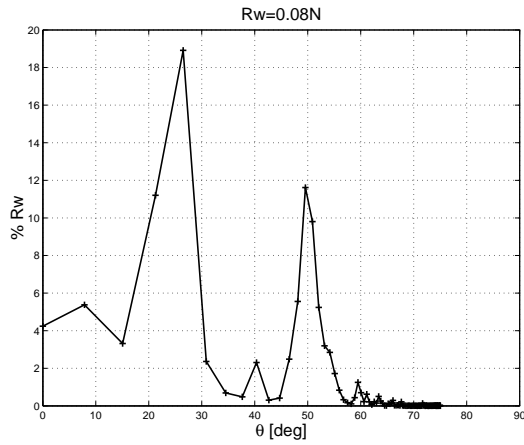


Figure 78: Model 6b: cat $S/L=0.2$, $V=1\text{m/s}$
 $H=400\text{mm}$

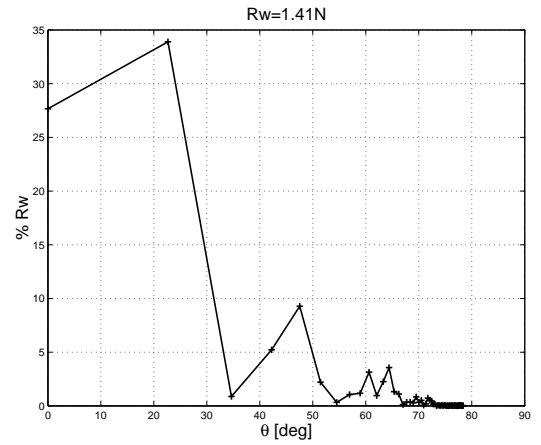


Figure 79: Model 6b: cat $S/L=0.2$,
 $V=1.7\text{m/s}$ $H=400\text{mm}$

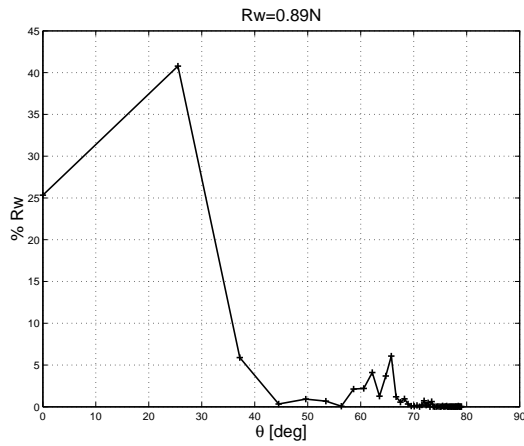


Figure 80: Model 6b: cat $S/L=0.2$,
 $V=1.8\text{m/s}$ $H=400\text{mm}$

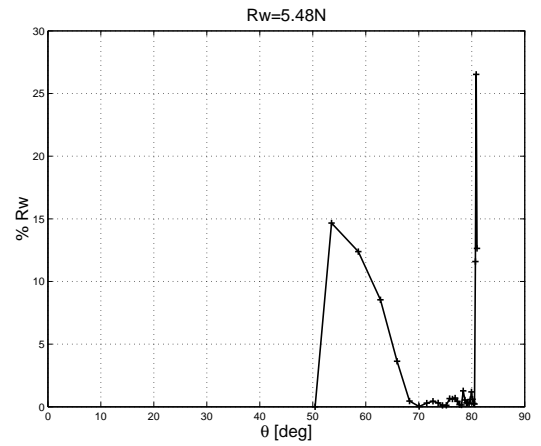


Figure 81: Model 6b: cat $S/L=0.2$, $V=3\text{m/s}$
 $H=400\text{mm}$

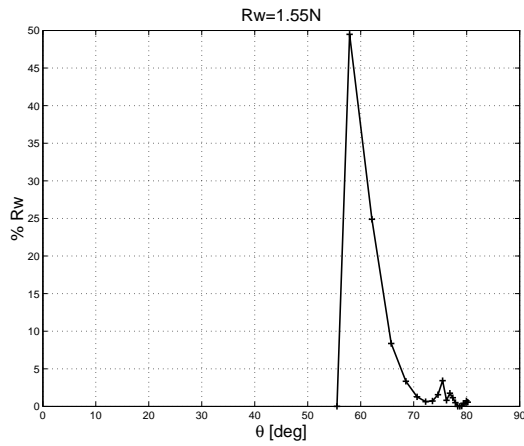


Figure 82: Model 6b: cat $S/L=0.2$,
 $V=3.5\text{m/s}$ $H=400\text{mm}$

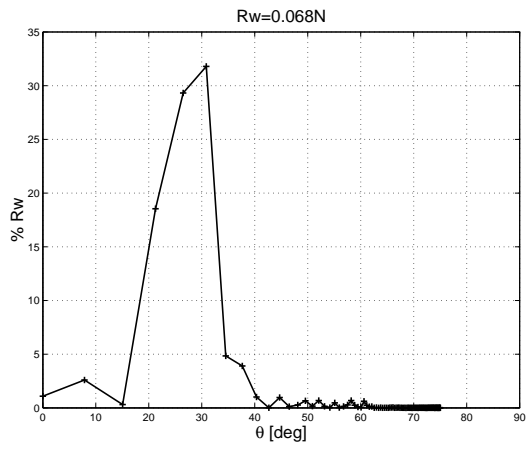


Figure 83: Model 5s: cat S/L=0.2, V=1m/s
H=400mm

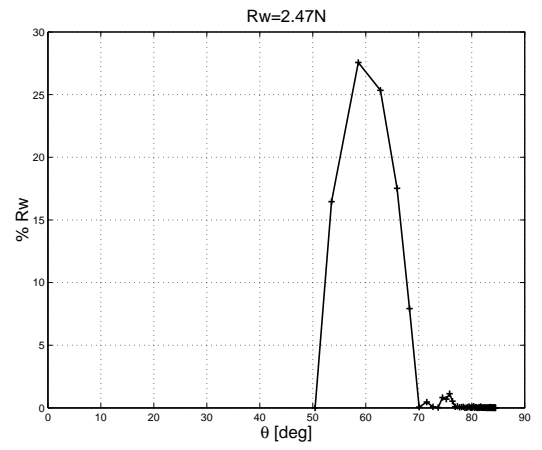


Figure 84: Model 5s: cat S/L=0.2, V=3m/s
H=400mm

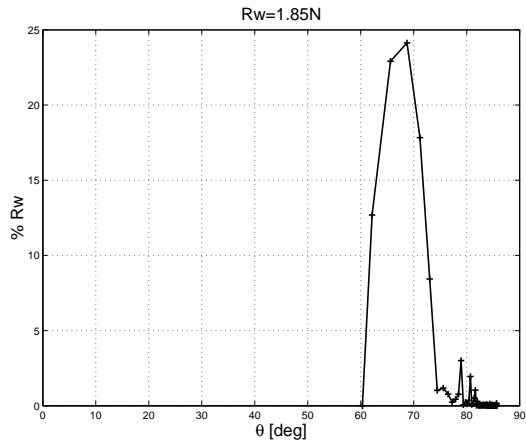


Figure 85: Model 5s: cat S/L=0.2, V=4m/s
H=400mm

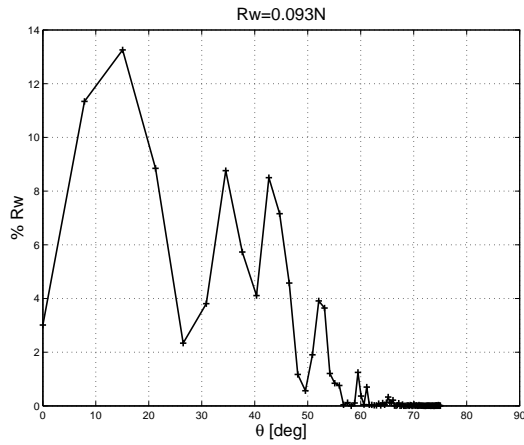


Figure 86: Model 4b: cat S/L=0.4, V=1m/s H=400mm

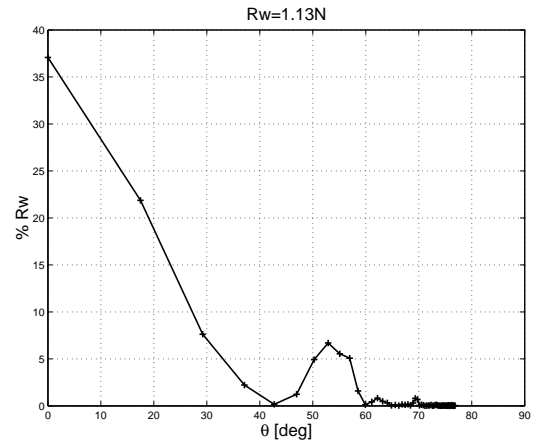


Figure 87: Model 4b: cat S/L=0.4, V=1.5m/s H=400mm

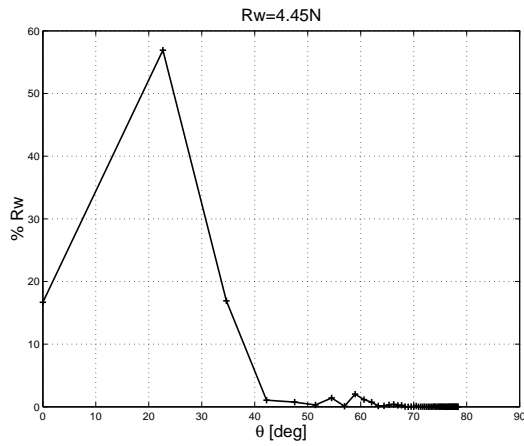


Figure 88: Model 4b: cat S/L=0.4, V=1.7m/s H=400mm

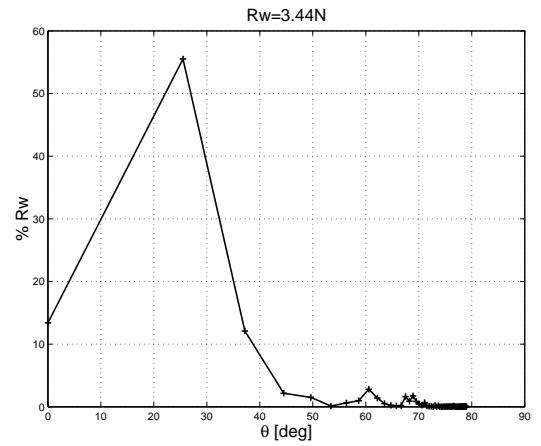


Figure 89: Model 4b: cat S/L=0.4, V=1.8m/s H=400mm

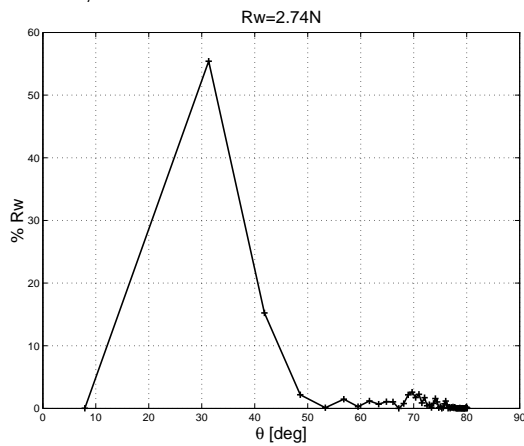


Figure 90: Model 4b: cat S/L=0.4, V=2m/s H=400mm

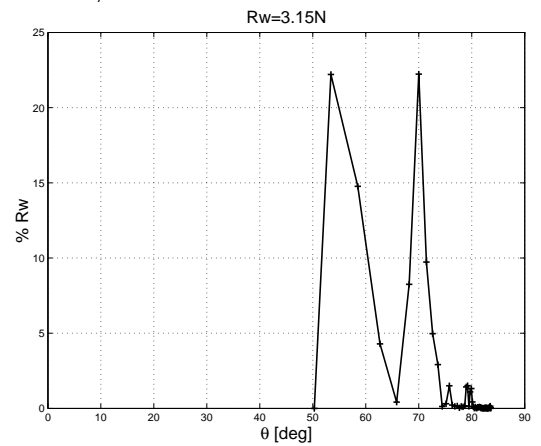


Figure 91: Model 4b: cat S/L=0.4, V=3m/s H=400mm

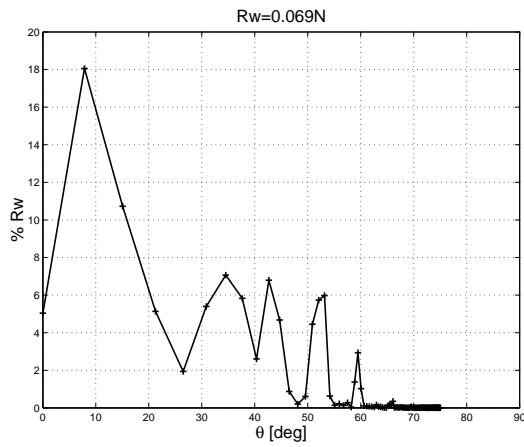


Figure 92: Model 5b: cat S/L=0.4, V=1m/s H=400mm

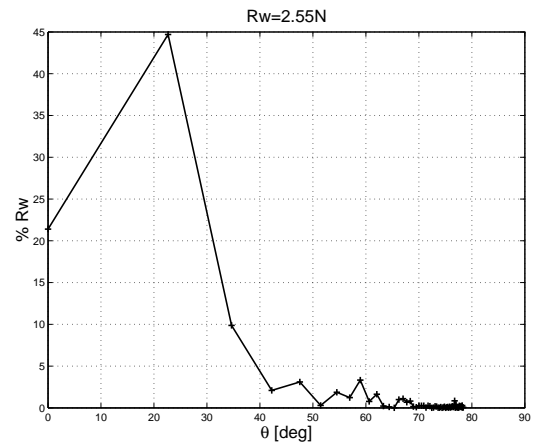


Figure 93: Model 5b: cat S/L=0.4, V=1.7m/s H=400mm

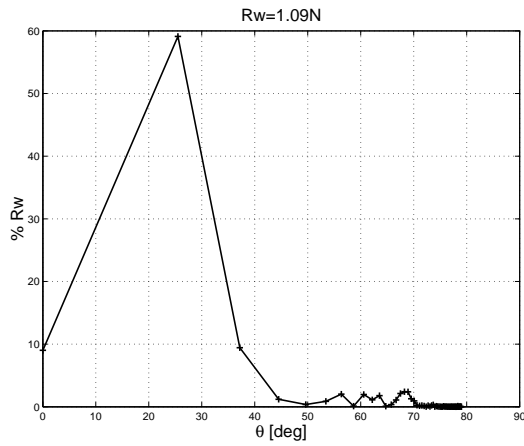


Figure 94: Model 5b: cat S/L=0.4, V=1.8m/s H=400mm

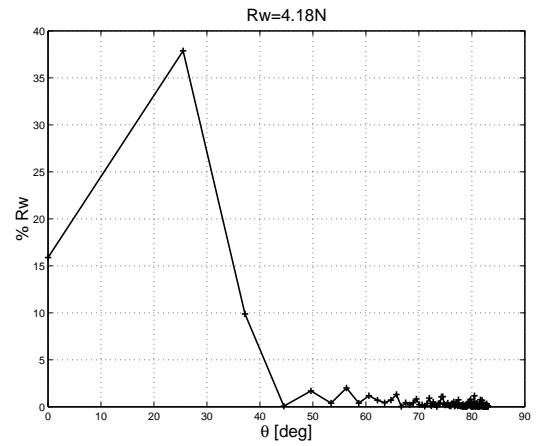


Figure 95: Model 5b: cat S/L=0.4, V=1.8m/s H=400mm

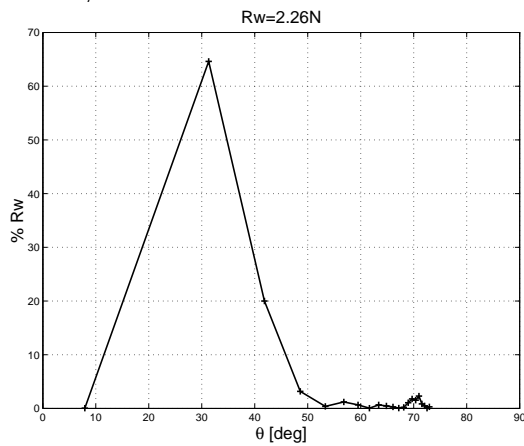


Figure 96: Model 5b: cat S/L=0.4, V=2m/s H=400mm

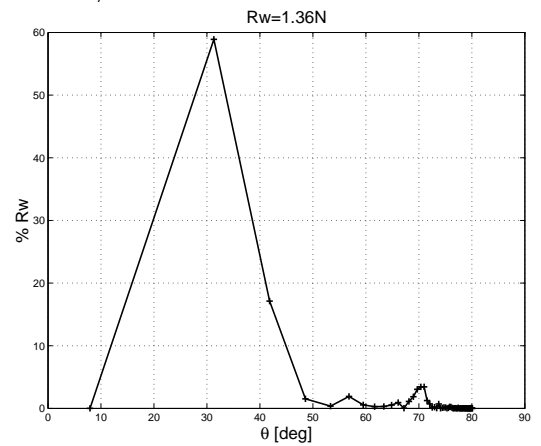


Figure 97: Model 5b: cat S/L=0.4, V=2m/s H=400mm

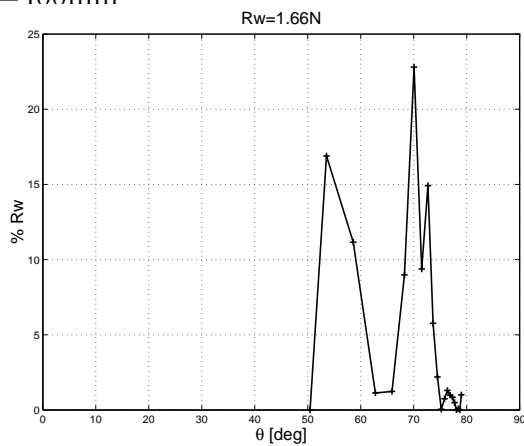


Figure 98: Model 5b: cat S/L=0.4, V=3m/s H=400mm

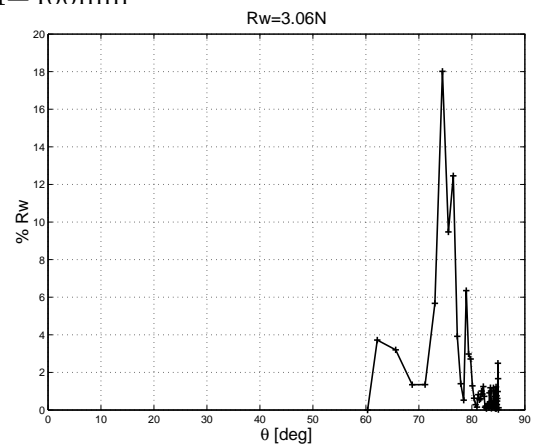


Figure 99: Model 5b: cat S/L=0.4, V=4m/s H=400mm

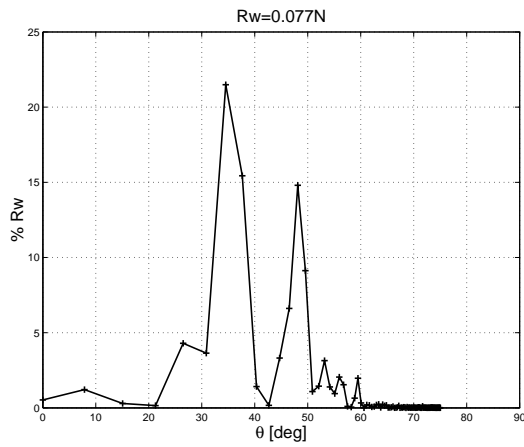


Figure 100: Model 6b: cat S/L=0.4, V=1m/s H=400mm

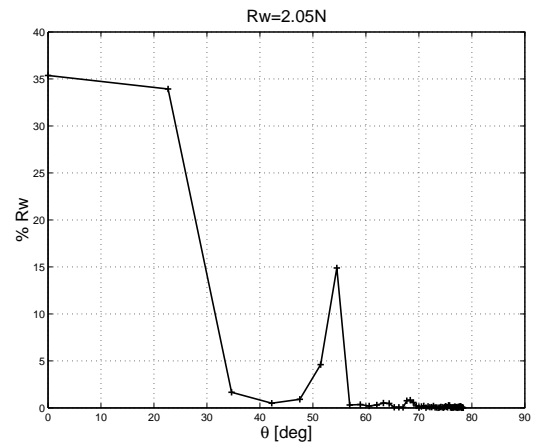


Figure 101: Model 6b: cat S/L=0.4, V=1.7m/s H=400mm

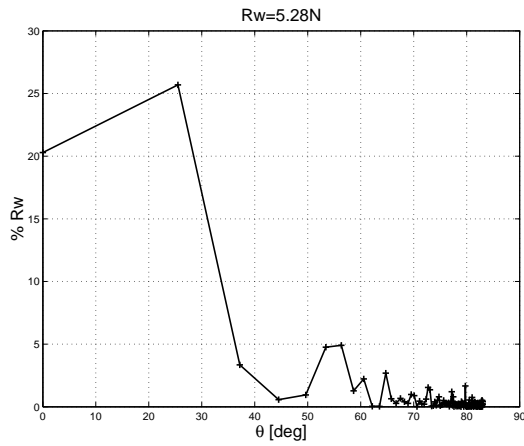


Figure 102: Model 6b: cat S/L=0.4, V=1.8m/s H=400mm

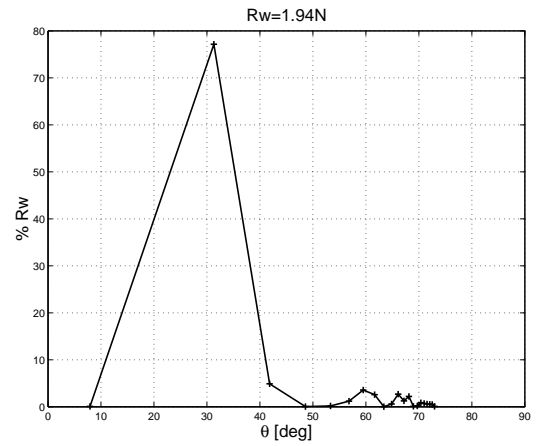


Figure 103: Model 6b: cat S/L=0.4, V=2m/s H=400mm

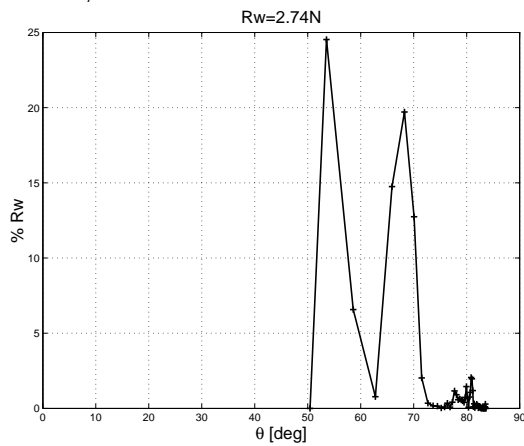


Figure 104: Model 6b: cat S/L=0.4, V=3m/s H=400mm

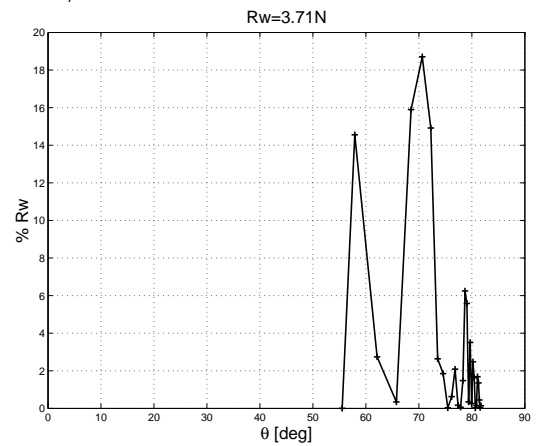


Figure 105: Model 6b: cat S/L=0.4, V=3.5m/s H=400mm

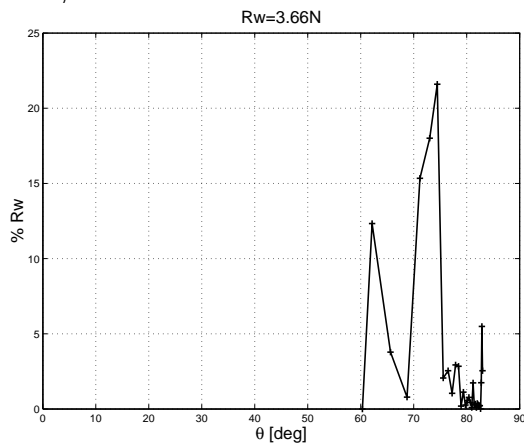


Figure 106: Model 6b: cat S/L=0.4, V=4m/s H=400mm

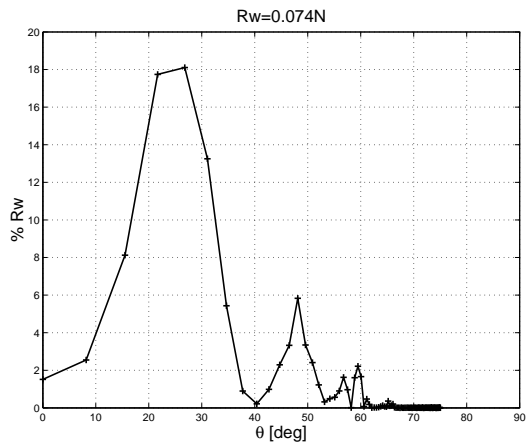


Figure 107: Model 4b: mono, $V=1\text{m/s}$
 $H=200\text{mm}$

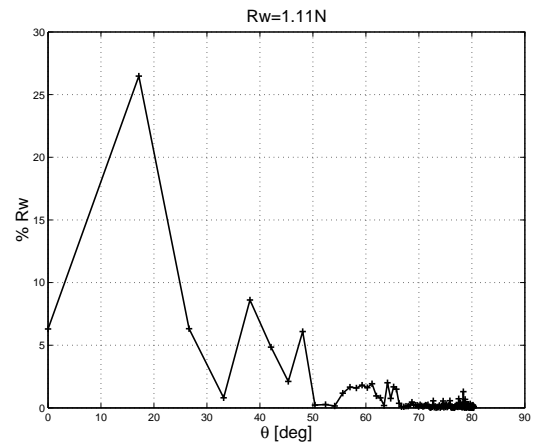


Figure 108: Model 4b: mono, $V=1.3\text{m/s}$
 $H=200\text{mm}$

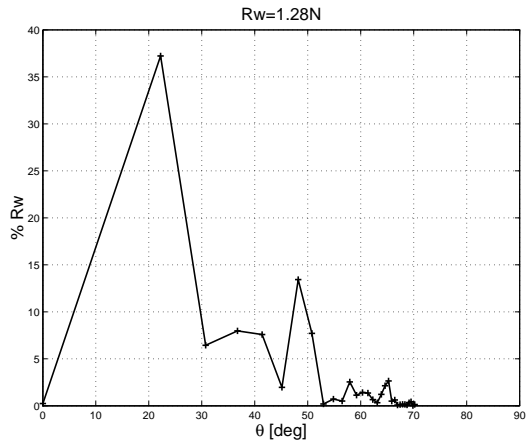


Figure 109: Model 4b: mono, $V=1.4\text{m/s}$
 $H=200\text{mm}$

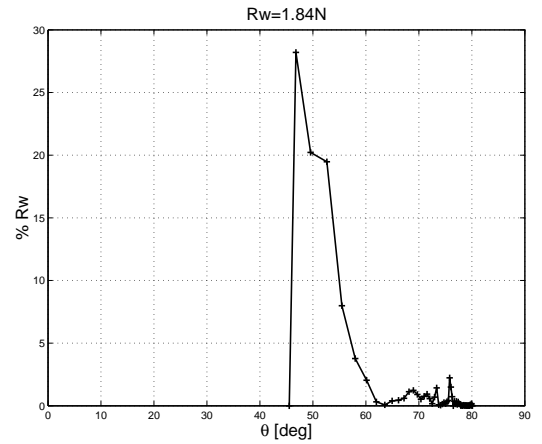


Figure 110: Model 4b: mono, $V=2\text{m/s}$
 $H=200\text{mm}$

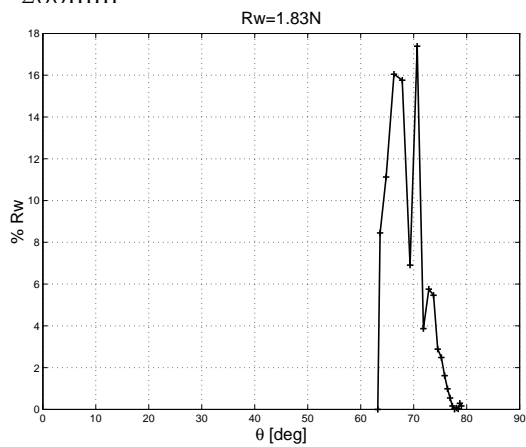


Figure 111: Model 4b: mono, $V=3\text{m/s}$
 $H=200\text{mm}$

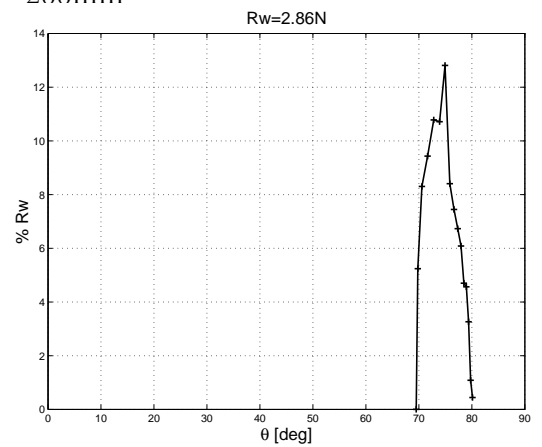


Figure 112: Model 4b: mono, $V=4\text{m/s}$
 $H=200\text{mm}$

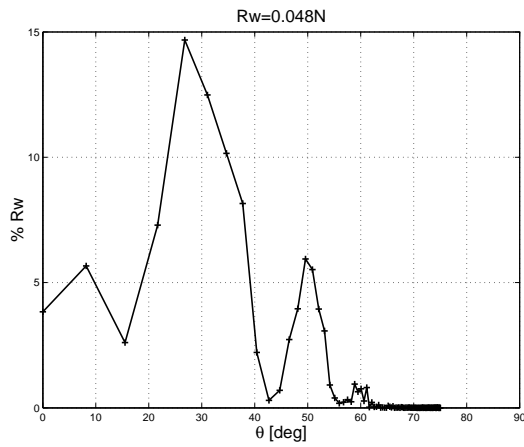


Figure 113: Model 5b: mono, $V=1\text{m/s}$
 $H=200\text{mm}$

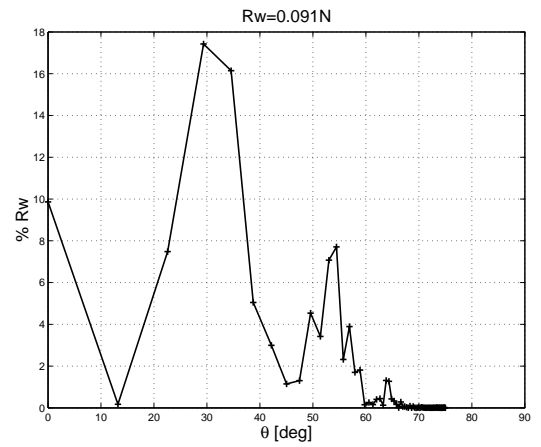


Figure 114: Model 5b: mono, $V=1.2\text{m/s}$
 $H=200\text{mm}$

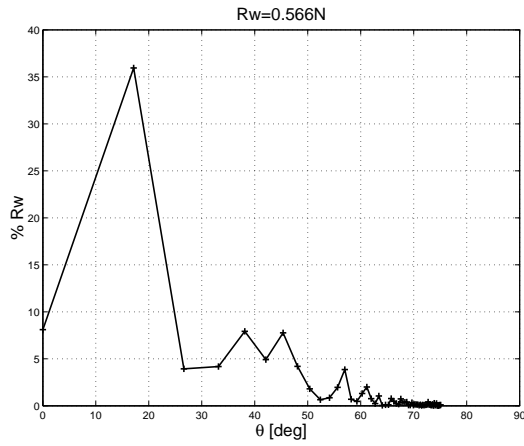


Figure 115: Model 5b: mono, $V=1.3\text{m/s}$
 $H=200\text{mm}$

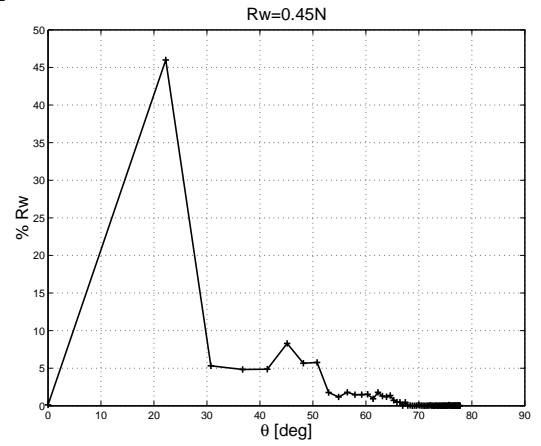


Figure 116: Model 5b: mono, $V=1.4\text{m/s}$
 $H=200\text{mm}$

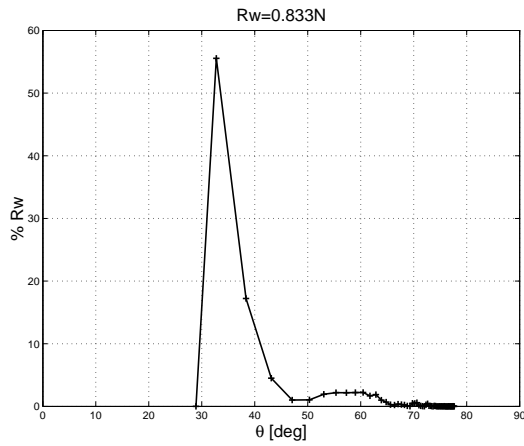


Figure 117: Model 5b: mono, $V=1.6\text{m/s}$
 $H=200\text{mm}$

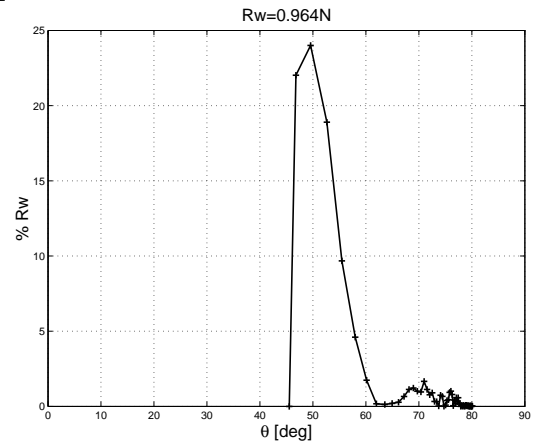


Figure 118: Model 5b: mono, $V=2\text{m/s}$
 $H=200\text{mm}$

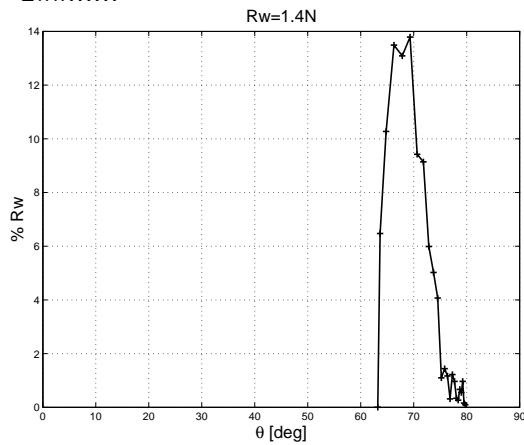


Figure 119: Model 5b: mono, $V=3\text{m/s}$
 $H=200\text{mm}$

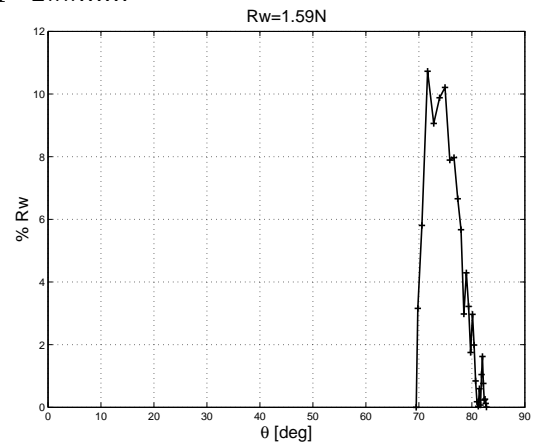


Figure 120: Model 5b: mono, $V=4\text{m/s}$
 $H=200\text{mm}$

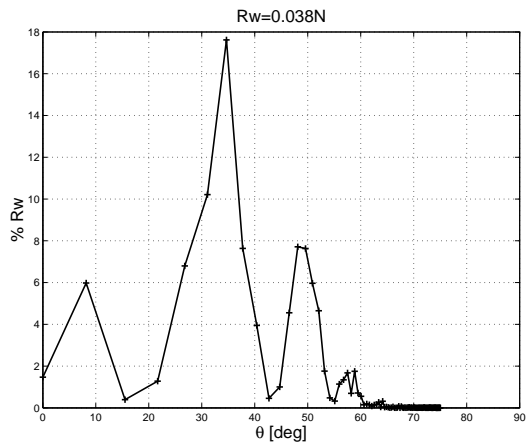


Figure 121: Model 6b: mono, $V=1\text{m/s}$
 $H=200\text{mm}$

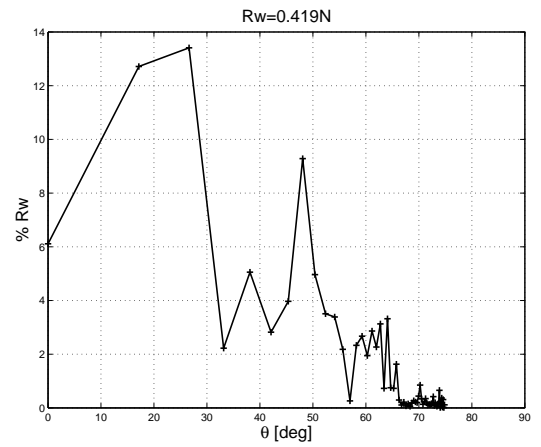


Figure 122: Model 6b: mono, $V=1.3\text{m/s}$
 $H=200\text{mm}$

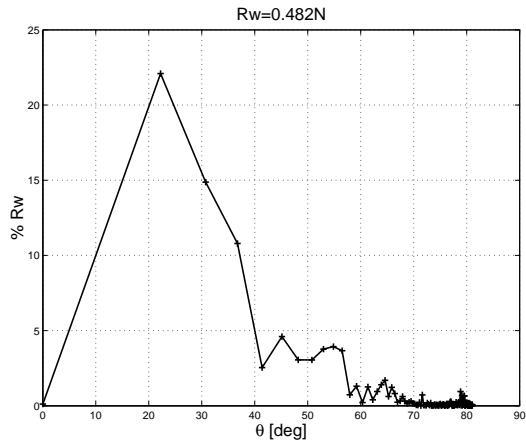


Figure 123: Model 6b: mono, $V=1.4\text{m/s}$
 $H=200\text{mm}$

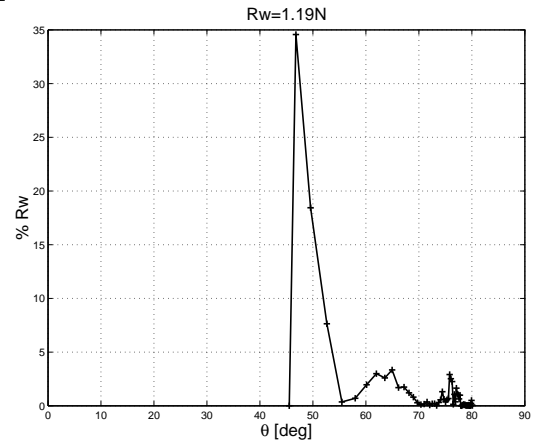


Figure 124: Model 6b: mono, $V=2\text{m/s}$
 $H=200\text{mm}$

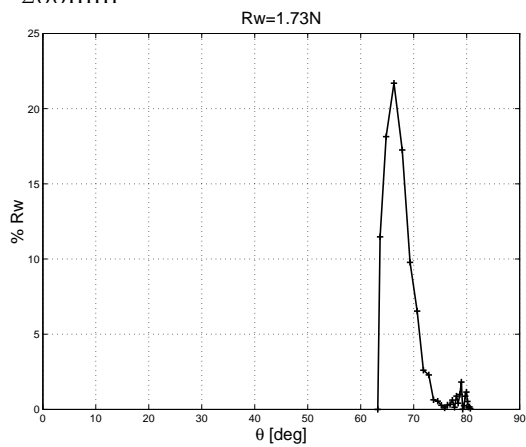


Figure 125: Model 6b: mono, $V=3\text{m/s}$
 $H=200\text{mm}$

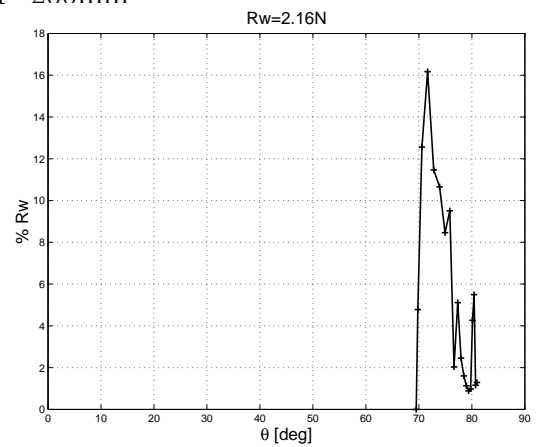


Figure 126: Model 6b: mono, $V=4\text{m/s}$
 $H=200\text{mm}$

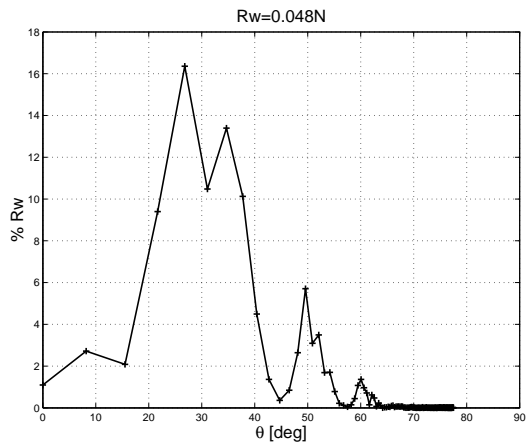


Figure 127: Model 5b: mono, $V=1\text{m/s}$
 $H=200\text{mm}$

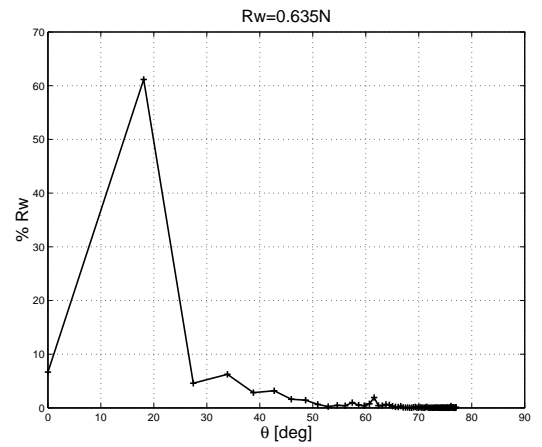


Figure 128: Model 5b: mono, $V=1.3\text{m/s}$
 $H=200\text{mm}$

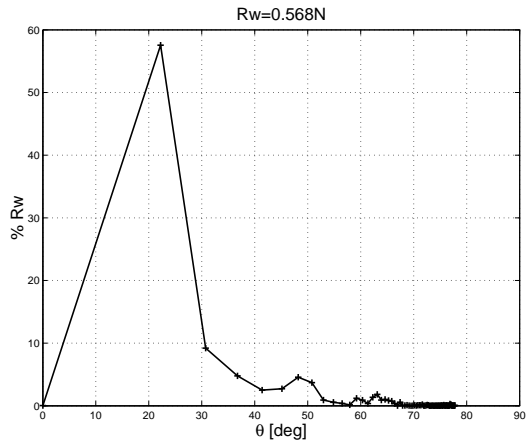


Figure 129: Model 5b: mono, $V=1.4\text{m/s}$
 $H=200\text{mm}$

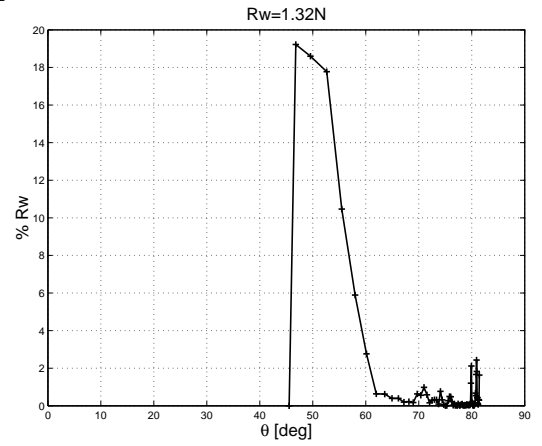


Figure 130: Model 5b: mono, $V=2\text{m/s}$
 $H=200\text{mm}$

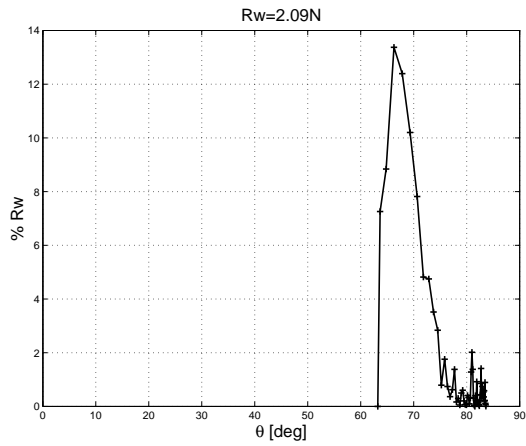


Figure 131: Model 5b: mono, $V=3\text{m/s}$
 $H=200\text{mm}$

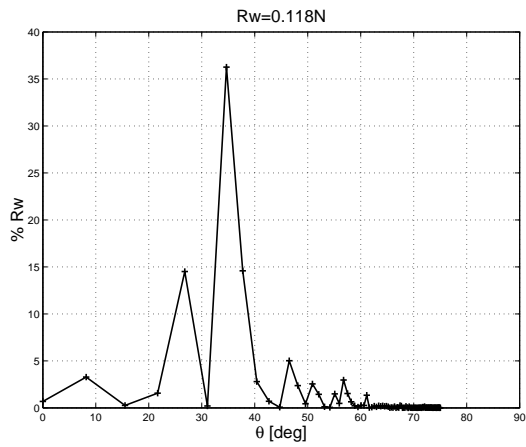


Figure 132: Model 4b: cat S/L=0.2, V=1m/s H=200mm

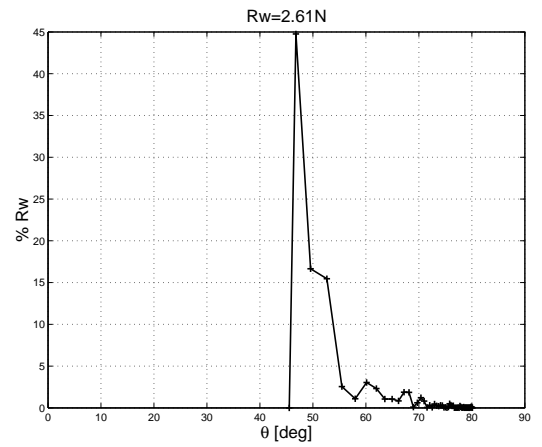


Figure 133: Model 4b: cat S/L=0.2, V=2m/s H=200mm

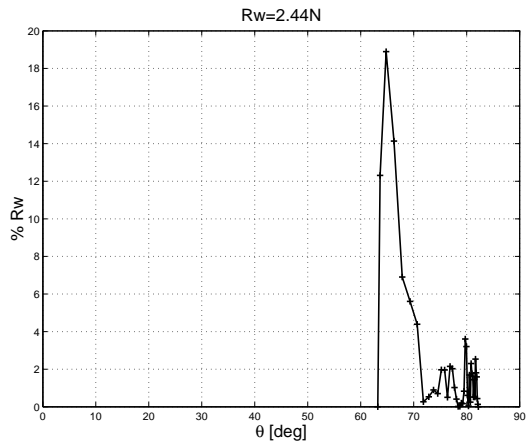


Figure 134: Model 4b: cat S/L=0.2, V=3m/s H=200mm

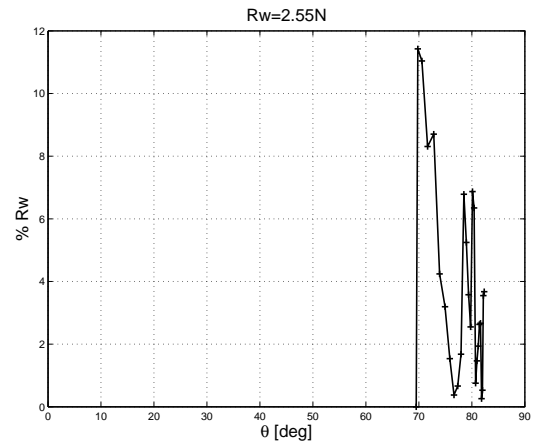


Figure 135: Model 4b: cat S/L=0.2, V=4m/s H=200mm

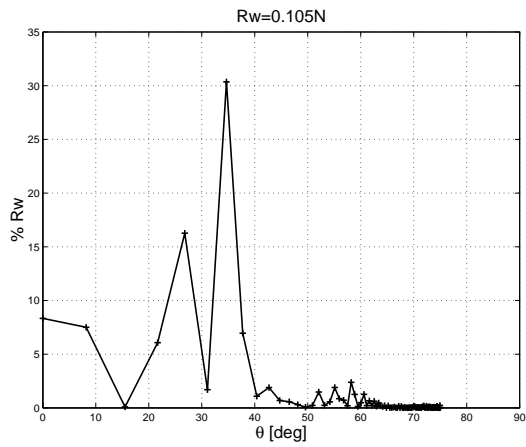


Figure 136: Model 5b: cat S/L=0.2, V=1m/s H=200mm

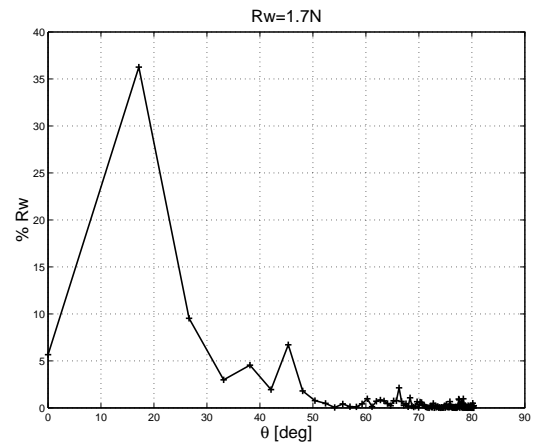


Figure 137: Model 5b: cat S/L=0.2, V=1.3m/s H=200mm

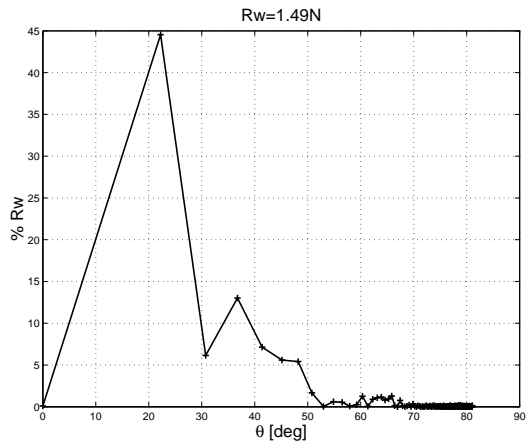


Figure 138: Model 5b: cat S/L=0.2, V=1.4m/s H=200mm

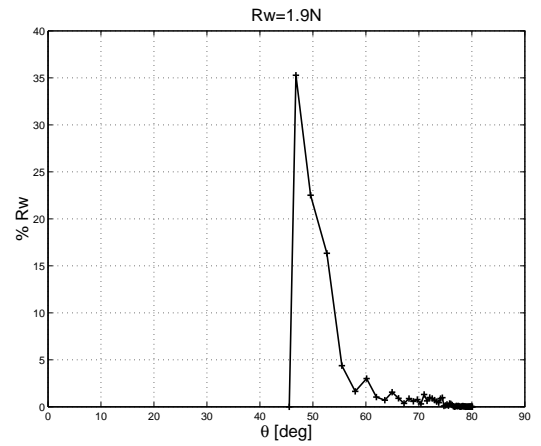


Figure 139: Model 5b: cat S/L=0.2, V=2m/s H=200mm

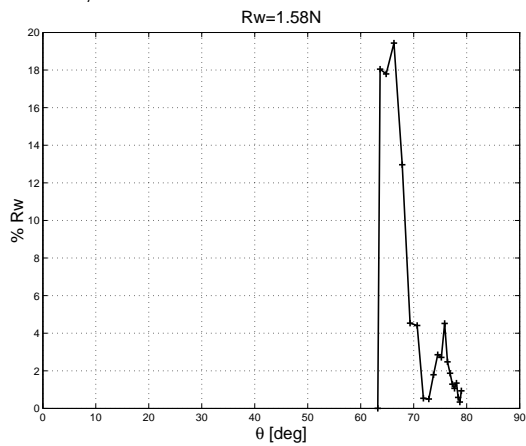


Figure 140: Model 5b: cat S/L=0.2, V=3m/s H=200mm

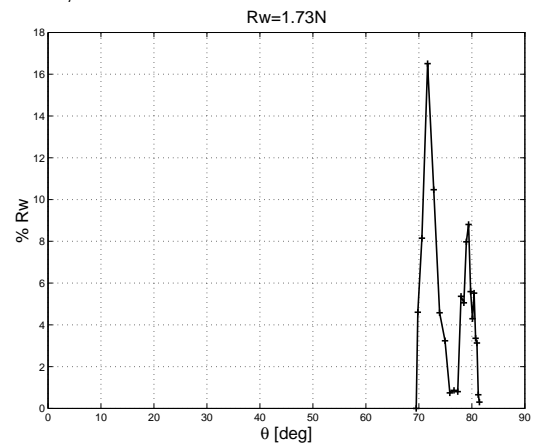


Figure 141: Model 5b: cat S/L=0.2, V=4m/s H=200mm

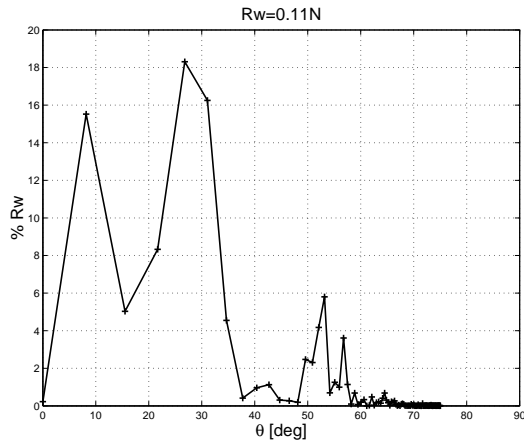


Figure 142: Model 6b: cat S/L=0.2, V=1m/s H=200mm

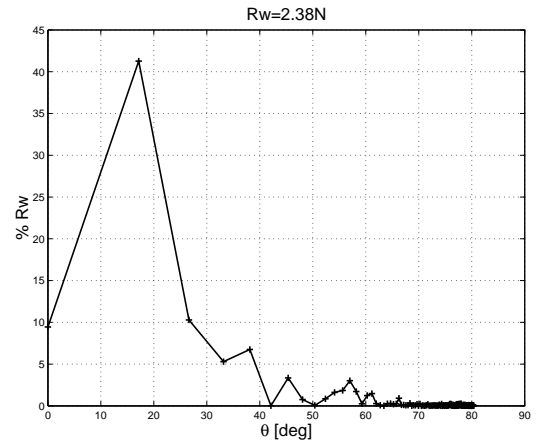


Figure 143: Model 6b: cat S/L=0.2, V=1.3m/s H=200mm

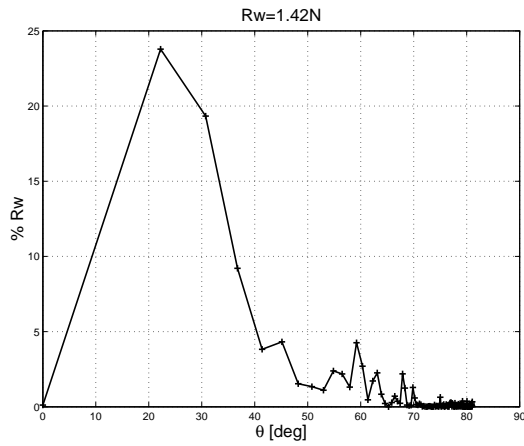


Figure 144: Model 6b: cat S/L=0.2, V=1.4m/s H=200mm

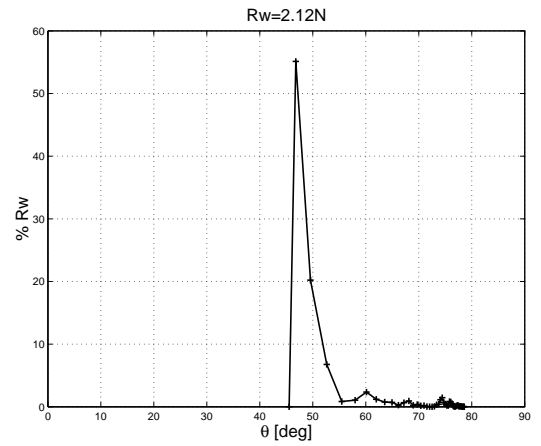


Figure 145: Model 6b: cat S/L=0.2, V=2m/s H=200mm

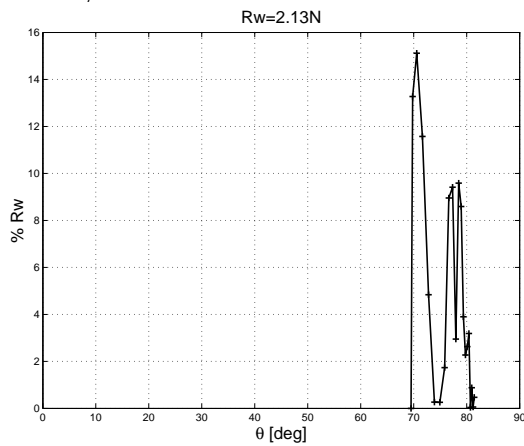


Figure 146: Model 6b: cat S/L=0.2, V=4m/s H=200mm

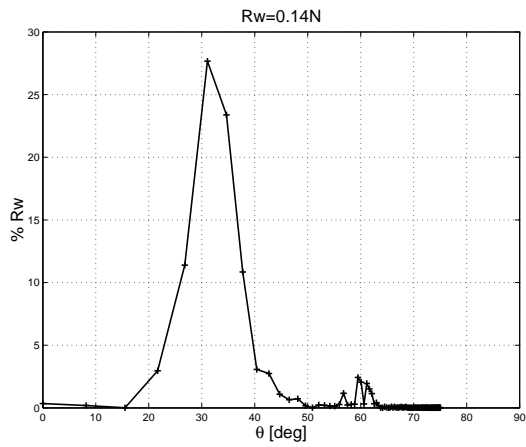


Figure 147: Model 5b: cat S/L=0.2, V=1m/s H=200mm

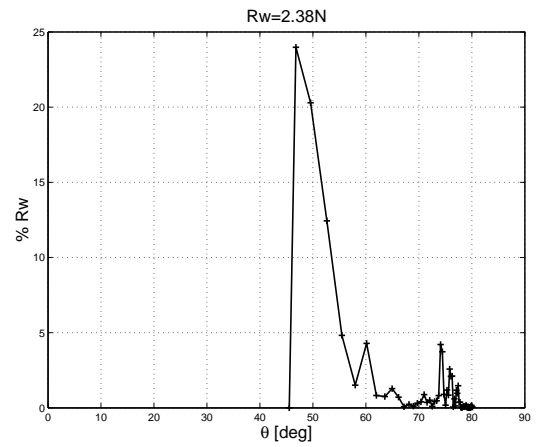


Figure 148: Model 5b: cat S/L=0.2, V=2m/s H=200mm

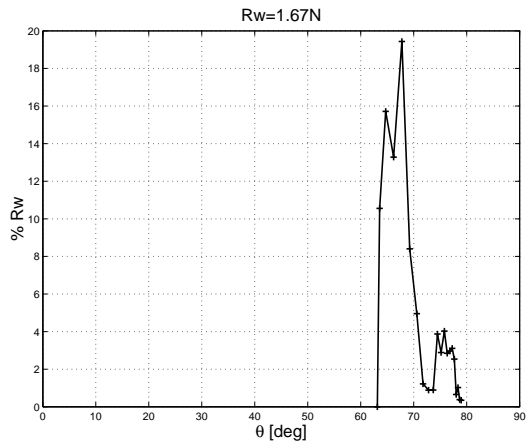


Figure 149: Model 5b: cat S/L=0.2, V=3m/s H=400mm

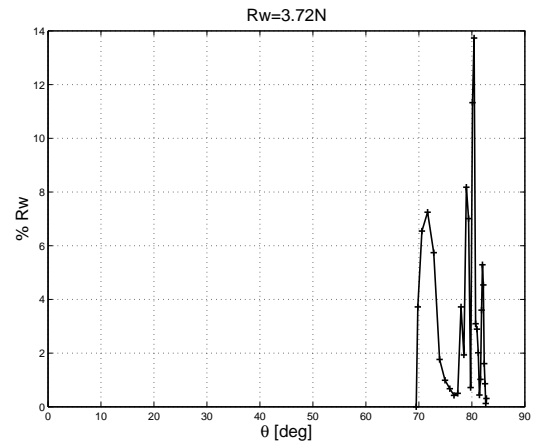


Figure 150: Model 5b: cat S/L=0.2, V=4m/s H=400mm

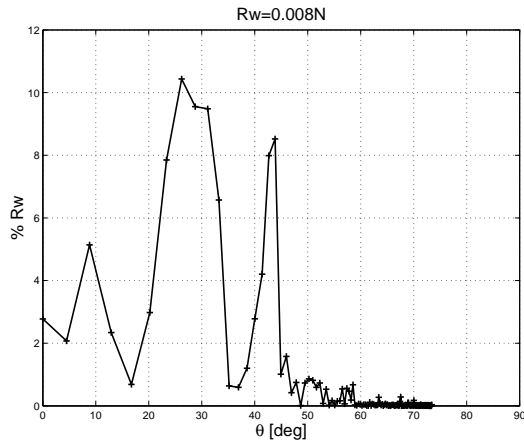


Figure 151: Model 4b: cat S/L=0.4, V=0.75m/s H=200mm

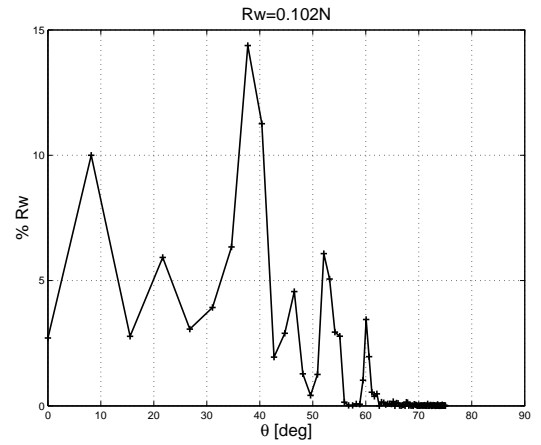


Figure 152: Model 4b: cat S/L=0.4, V=1m/s H=200mm

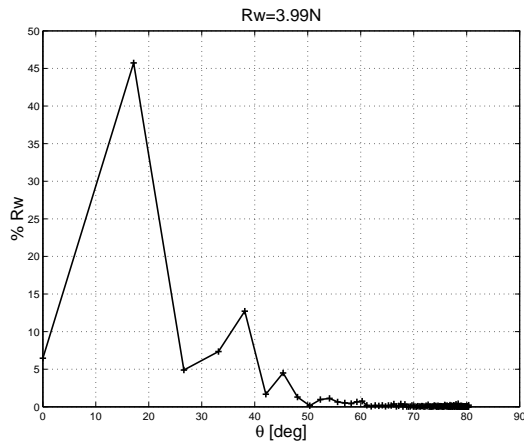


Figure 153: Model 4b: cat S/L=0.4, V=1.3m/s H=200mm

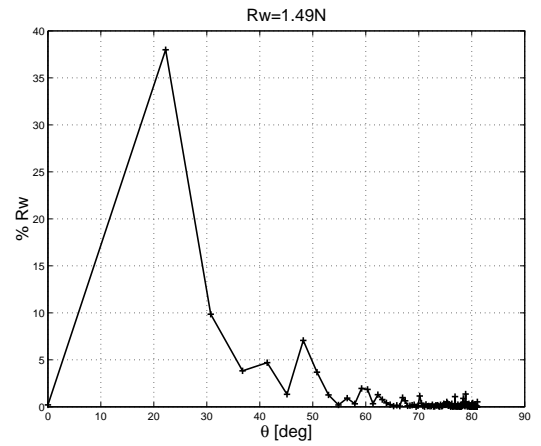


Figure 154: Model 4b: cat S/L=0.4, V=1.4m/s H=200mm

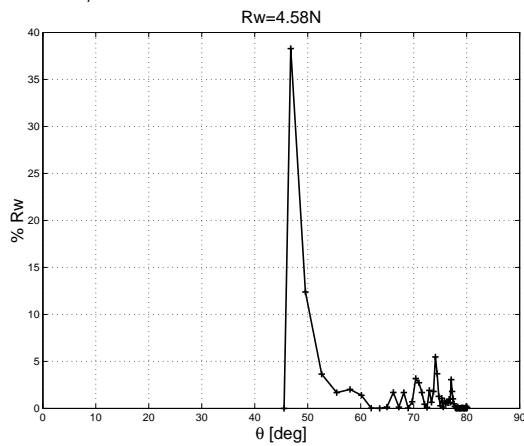


Figure 155: Model 4b: cat S/L=0.4, V=2m/s H=200mm

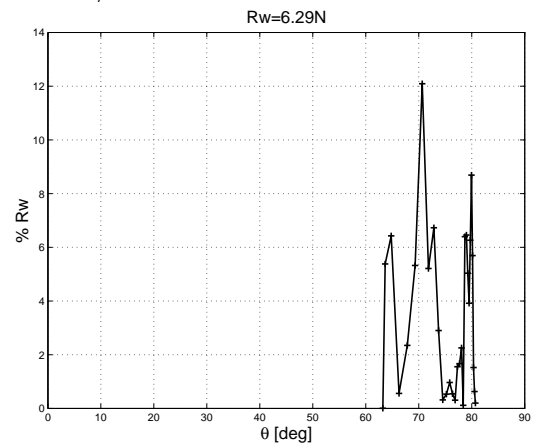


Figure 156: Model 4b: cat S/L=0.4, V=3m/s H=200mm

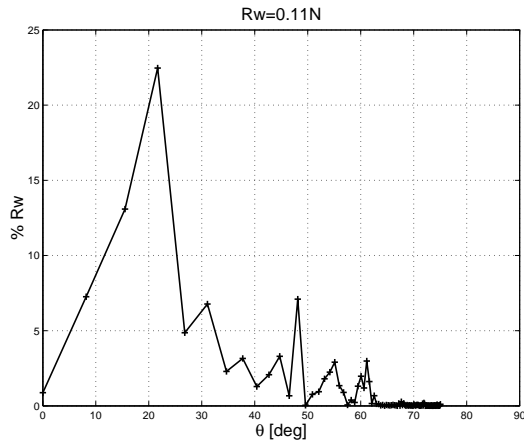


Figure 157: Model 5b: cat S/L=0.4, V=1m/s H=200mm

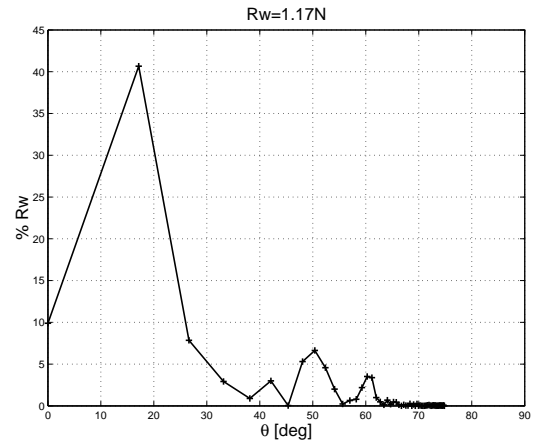


Figure 158: Model 5b: cat S/L=0.4, V=1.3m/s H=200mm

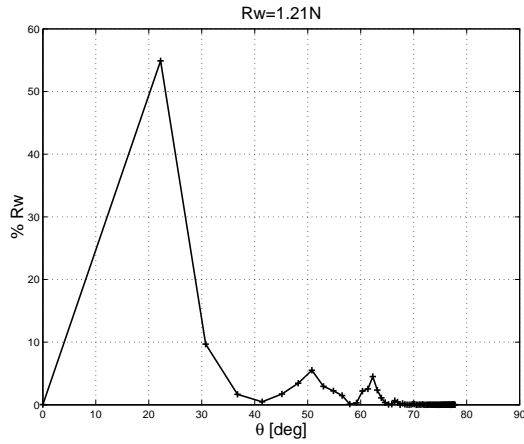


Figure 159: Model 5b: cat S/L=0.4, V=1.4m/s H=200mm

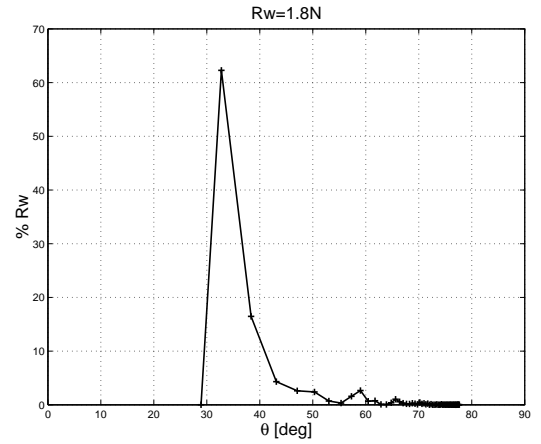


Figure 160: Model 5b: cat S/L=0.4, V=1.6m/s H=200mm

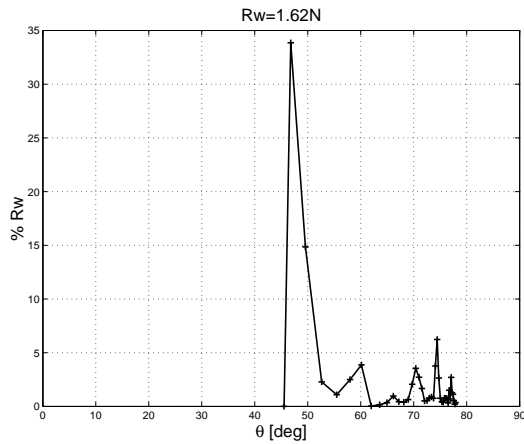


Figure 161: Model 5b: cat S/L=0.4, V=2m/s H=200mm

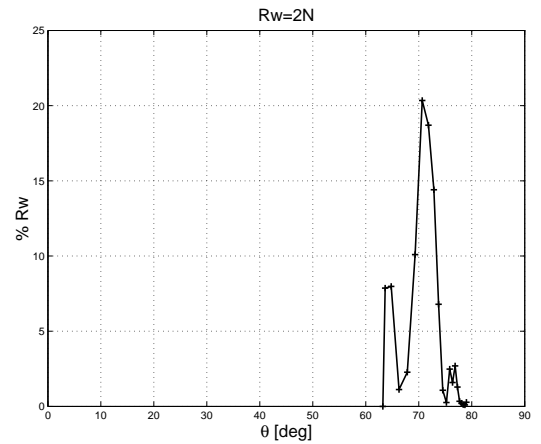


Figure 162: Model 5b: cat S/L=0.4, V=3m/s H=200mm

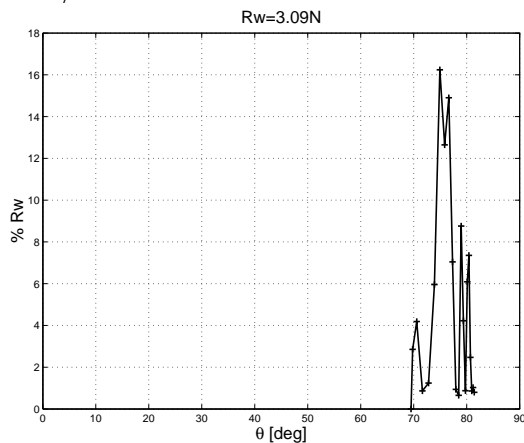


Figure 163: Model 5b: cat S/L=0.4, V=4m/s H=200mm

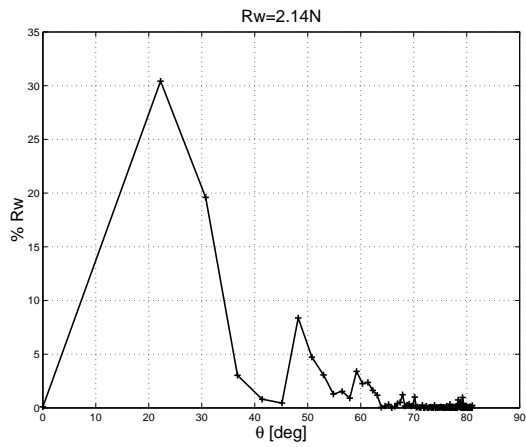


Figure 164: Model 6b: cat S/L=0.4, V=1.4m/s H=200mm

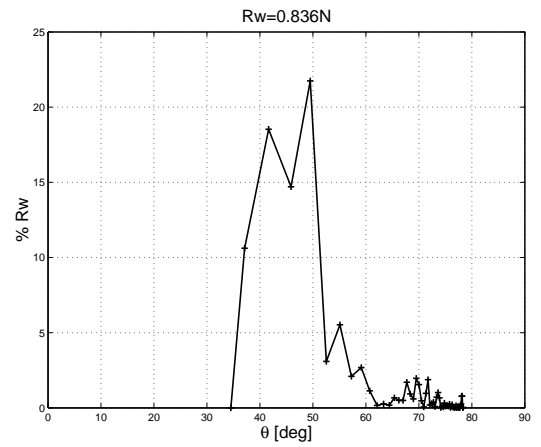


Figure 165: Model 6b: cat S/L=0.4, V=1.7m/s H=200mm

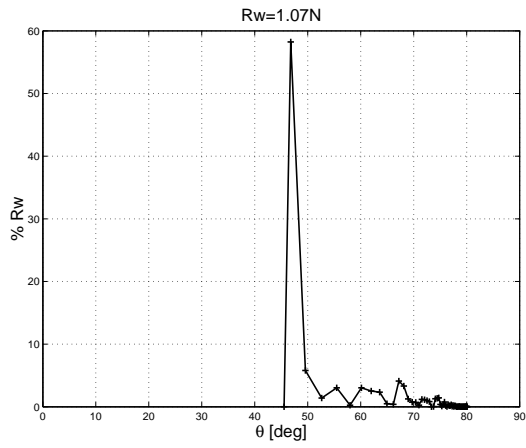


Figure 166: Model 6b: cat S/L=0.4, V=2m/s H=200mm

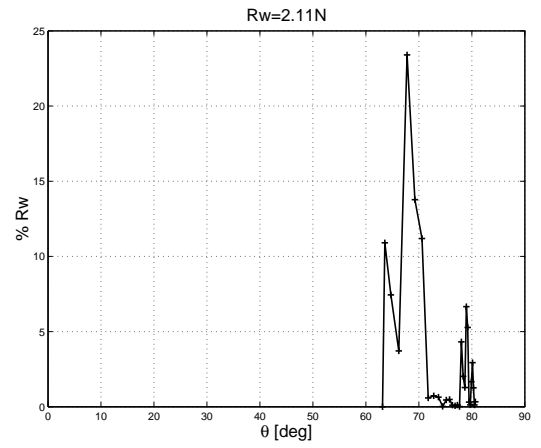


Figure 167: Model 6b: cat S/L=0.4, V=3m/s H=200mm

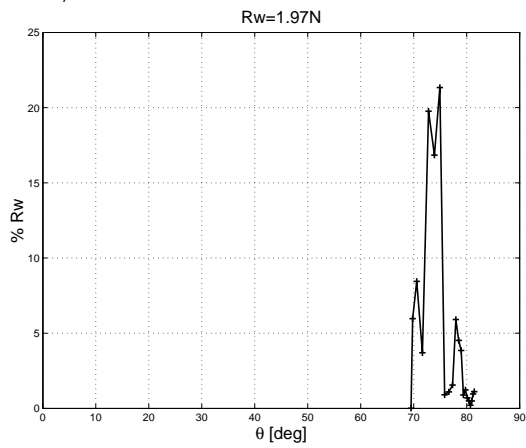


Figure 168: Model 6b: cat S/L=0.4, V=4m/s H=200mm

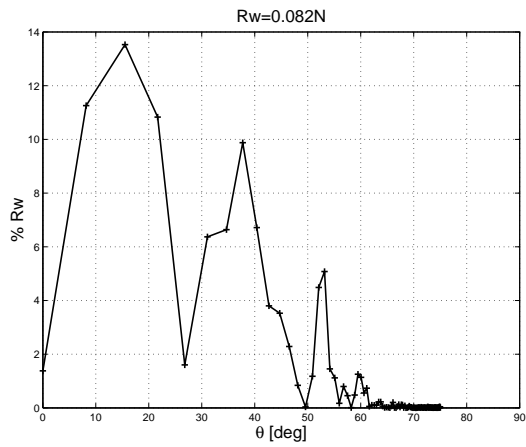


Figure 169: Model 5s: cat S/L=0.4, V=1m/s
H=200mm

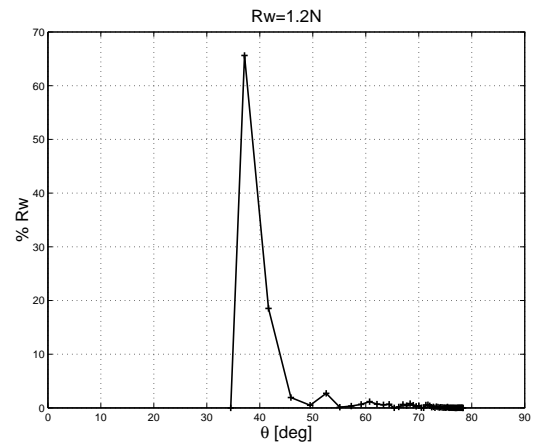


Figure 170: Model 5s: cat S/L=0.4,
V=1.7m/s H=200mm

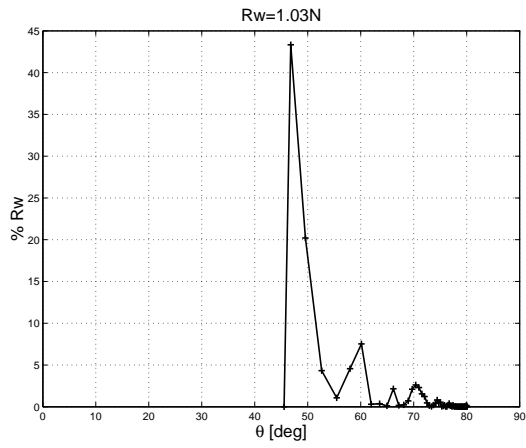


Figure 171: Model 5s: cat S/L=0.4, V=2m/s
H=200mm

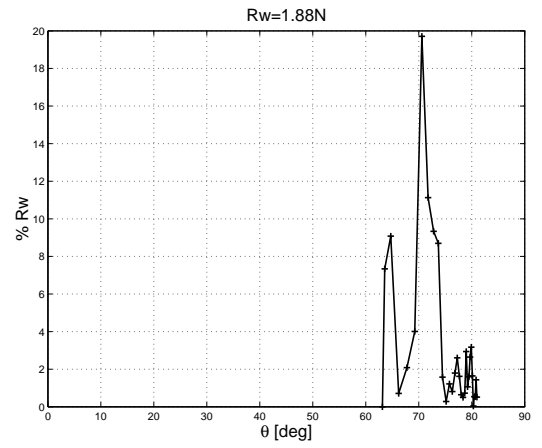


Figure 172: Model 5s: cat S/L=0.4, V=3m/s
H=200mm

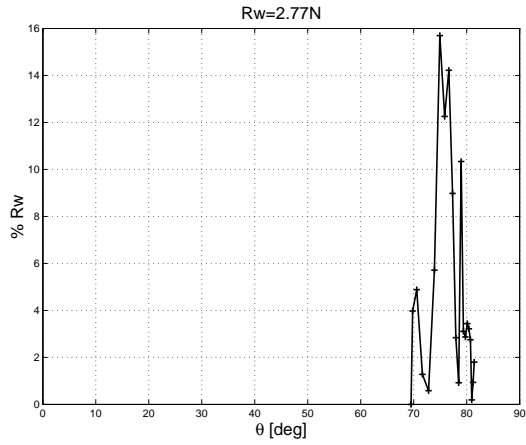


Figure 173: Model 5s: cat S/L=0.4, V=4m/s
H=200mm